



Supplement of

Evolution of squall line variability and error growth in an ensemble of large eddy simulations

Edward Groot and Holger Tost

Correspondence to: Edward Groot (egroot@uni-mainz.de)

The copyright of individual parts of the supplement might differ from the article licence.

Tracer concentrations: PT2 plots (Section 3.2.2)

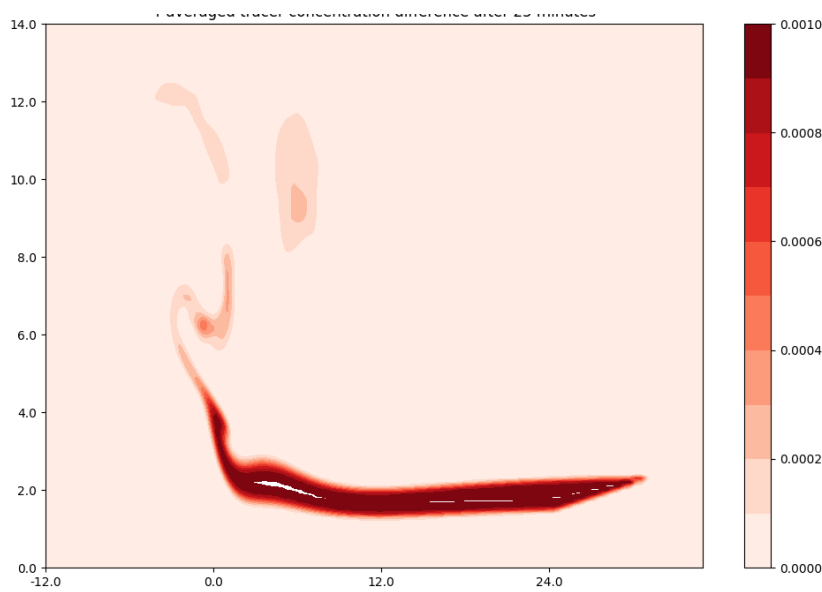


Figure S1. PT2 concentration after 25 minutes in reference simulation.

The plot above shows the concentration of passive tracer PT2 after 25 minutes of simulation in the reference simulation (in x-z cross section, averaged along the squall line). It was initialised in the region where $0 < x < 30$ km at levels of 1600-2400 m. The tracer is mostly still present in this region, while the easterly winds have advected it slightly westward. This leads to upward transport by the updrafts, which are approximately in the region $-3 < x < 3$ km. Concentrations are particularly high at the inflow of the updraft (near $x = 0$ km and $z = 3$ km). Some undulations occur between $0 < x < 10$ km, caused by gravity waves, moving layers vertically by a few hundred meters.

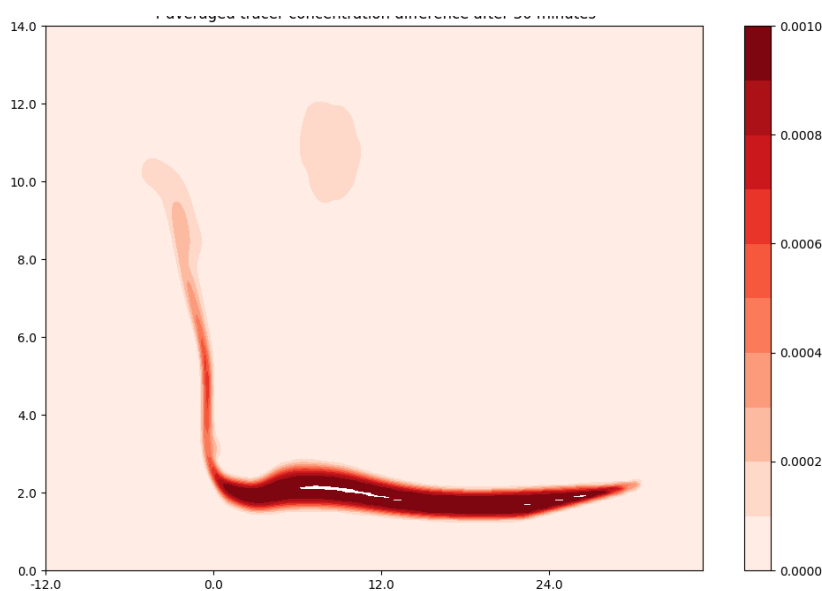


Figure S2. PT2 concentration after 30 minutes in reference simulation.

The next plot, Figure S2, represents the same tracer concentration as the previous plot (Figure S1), but then for 5 minutes later. The updraft is aligning more upright vertically and enhanced

concentrations reach higher altitudes. Furthermore, the undulating wave pattern has moved by a few kilometres. On the next page we add one ensemble member's PT2 concentration.

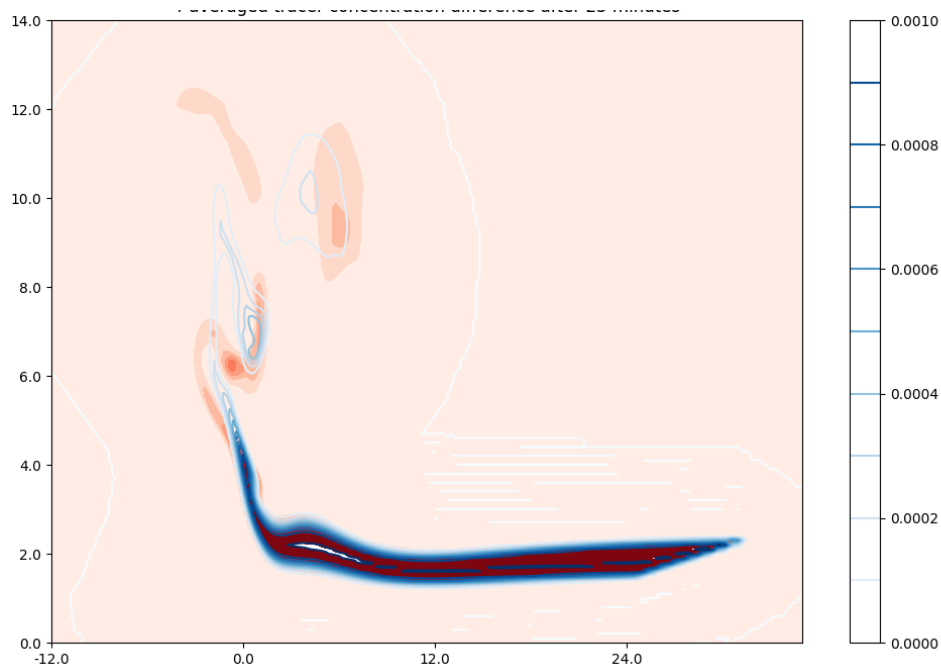


Figure S3. Same as Figure S2, but now blue isolines are superposed at concentrations given in the colour bar.

In Figure S3 the blue isolines and red fill overlap strongly at low levels. However, at mid-levels and in the upper troposphere differences occur: in the reference simulation, PT2 shifts slightly westward compared to ENS_03 at mid-levels (4-7 km). This shift is probably associated with a difference in updraft location. Differences are also visible in the upper troposphere, due to differences in location of tracer outflow. These differences are essentially nothing else than displacements of PT2 in the two simulations, as shown in Figures 4b, 4c, 4d and 5a and 5b in the main text.

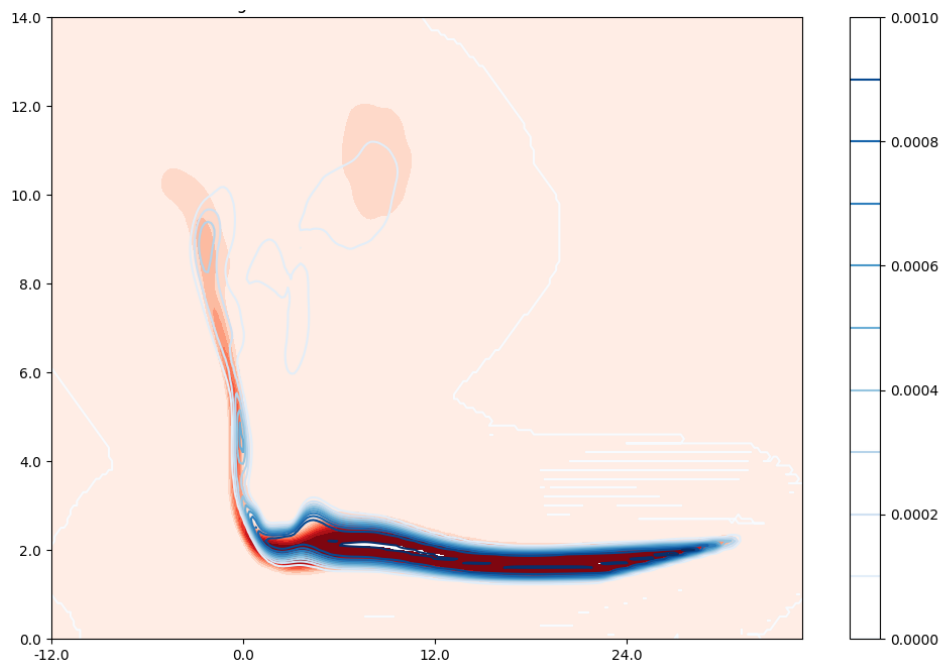


Figure S4. Same as Figure S3, but now for 30 minutes

Figure S4 represents the PT2 distribution in the reference simulation and ENS_03. There is a strong overlap in tracer distribution between the two simulations: the undulating signal at low levels, $z = 1600$ to $z = 2400$ m and $0 < x < 30$ km. The nearly upright updraft also occurs in both at about $x = 0$ km. However, when one focusses on the gradients of concentration one can also see that there are slight shifts between the two simulations: the updraft is very slightly shifted to the west in ENS_03 (blue isolines) than in the reference (red filled). Furthermore, whereas there is near perfect overlap in the region $5 < x < 30$ km at low levels, this is not the case directly east of the updraft at $0 < x < 5$ km. There is the pattern tracer PT2 has moved upward in the form of a crest-like pattern in ENS_03 and not in the reference simulation. This pattern is emphasized with the difference concentration plots, as given in Figures 4b, 4c, 4d, 5a and 5b.

Upper tropospheric patterns visible in PT1 and PT2 (Figure 5 of the main text)

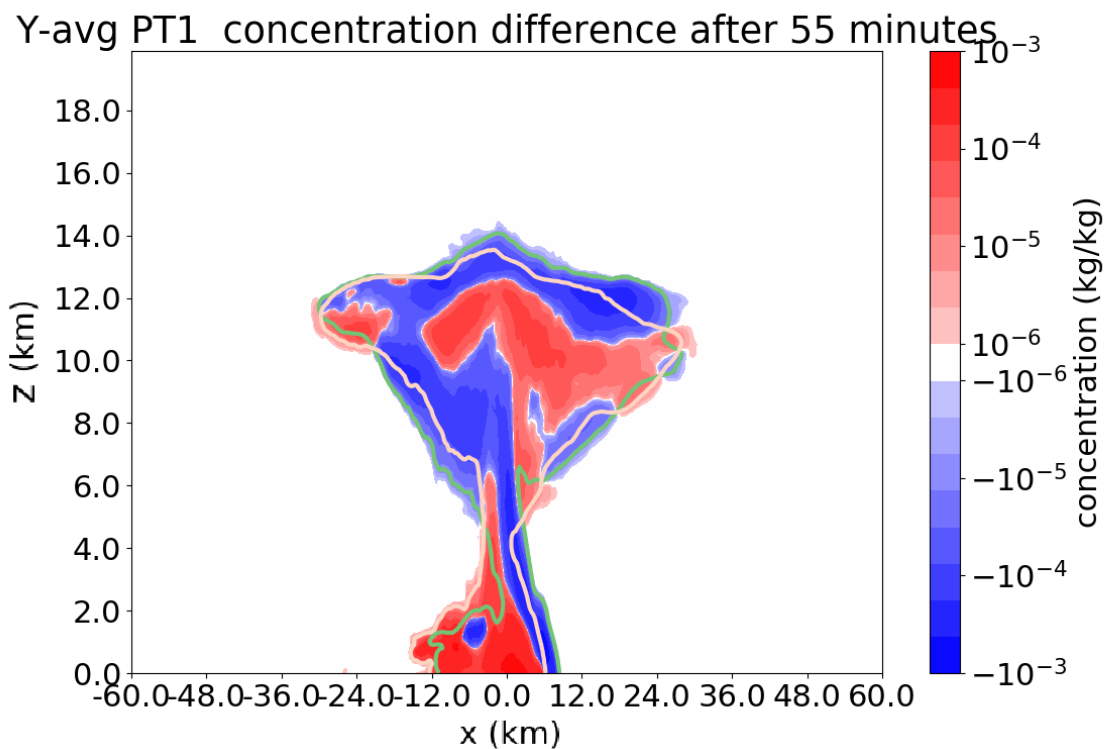


Figure S5. Copy of Figure 5a of the main text.

Both PT1 and PT2 (not shown, similar patterns) indicate that the top of the region with lower tropospheric tracers is lower in the reference simulation compared to the ENS-03. As the passive tracers are initiated at the location of source air for the convection, they reveal the source region of convected mass.

Two additional patterns are visible in Figure 5 of the main text:

1. The tracer is laterally spread out further in ENS-03 (green contour, Figure 5b) than in the reference simulation. Associated with that, the upper tropospheric divergence as visually demonstrated by the passive tracers is strongly increased in the ENS-03 (green) after 75 minutes compared to the reference. Upper tropospheric mass divergence averaged over a rectangular box volume around the system up to 75 minutes differs by 38% between the simulation pair, whereas the net latent heating left behind is only 24% higher in ENS-03 than in the reference simulation over the corresponding surface.

2. The overshooting top above $x = -5$ km is at higher altitude in ENS-03 (green) than in the reference simulation (bright colour, salmon/pink/orange).

These two patterns (Figure 5, main text) are a consequence of differential mass transport within the convection. Together with the patterns seen in PT2 earlier (main text, Section 3.2.2), increased convective overturn in ENS-03 may lead to all of the three patterns. Extra mass overturn is consistent with the reflectivity patterns in Section 3.1 of the main text.

Hovmöller diagrams of cold pool intensity

See the next page!

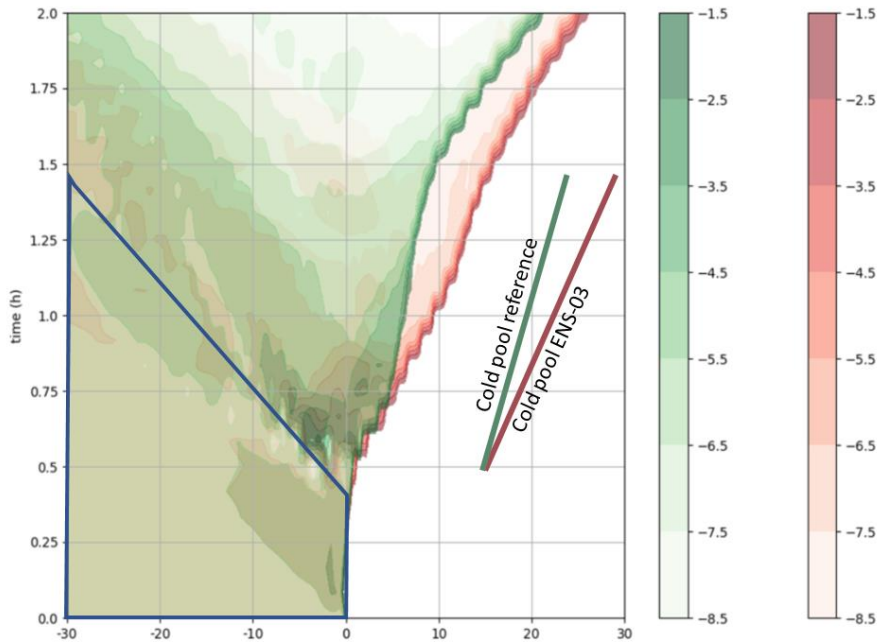


Figure S6a. Mean cold pool intensity at the surface as a function of x and t along a 10 km subsection of the squall line in the reference simulation and ENS-03.

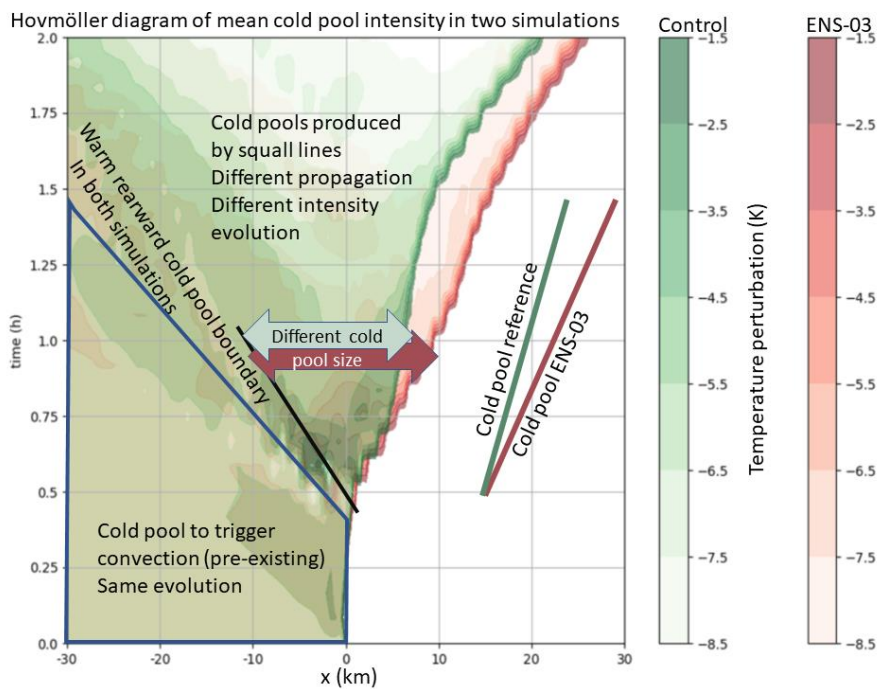


Figure S6b. Same, as Figure S6a, with additional annotations.

In Figure S6 one can see the area covered by cold pools grows in ENS-03 and the reference as a function of time. The cold pool in ENS-03 accelerates faster after 30 minutes than in the reference simulation, while the back side/rear flank of the newly generated cold pool (black line) coincides for both simulations. This means that the cold pool area of the newly generated cold pool grows faster in ENS-03 than in the reference case (light green; reference and dark red arrow; ENS-03). Note that the amplitude of the cold pools also evolves with time, as a response to variable precipitation intensities,

evaporation and other tendencies. However, one can see that the increase of the cold pool area coincides with an increase in the available space for cooling downdrafts in the Figure S6b.

Convergence and divergence: gravity wave signals

(Figure 3, main text, additional description of patterns in Figure 3, Section 3.2.1)

In addition to the main low level convergence features (listed in Section 3.2.1; Figure S7 in this supplement), convergence and divergence patterns associated with gravity waves are also visible in Figure 3/S7. These comparatively weak waves lose amplitude in time. Apparent intermittent behaviour in both figures for the western half of the domain is probably caused by the output interval of 5 minutes, approximately the apparent pulse frequency of these features.

Furthermore, the consequences of developing convective cells (Section 3.1) are visible only after the first 15 minutes. Lastly, as in the lower troposphere, one can also see patterns associated with comparatively weak gravity waves propagating in the upper troposphere, originating from the initial and secondary convective cells, which leave the model domain after the first hour.

Cold pool sensitivity to resolution

It has been noted that cold pool propagation and evaporation processes may be sensitive to resolution: cold pool dynamics might be affected by processes on smaller scales, such that they cannot be properly resolved with a layer thickness of 100m

Sub-optimal representation of shallow layer microphysics and cold pool dynamics will possibly induce similar biases among all ensemble members. Having executed a simulation at 50m vertical resolution with (supposedly) improved cold pool representation, the reproduced Figure 3 in the main text of the new simulation is very similar to the original Figure 3, with (in terms of details). Intermediate behaviour between the control simulation and ENS-03. Figure 3 and the similar Figure of the new simulation is provided below (Figure S7).

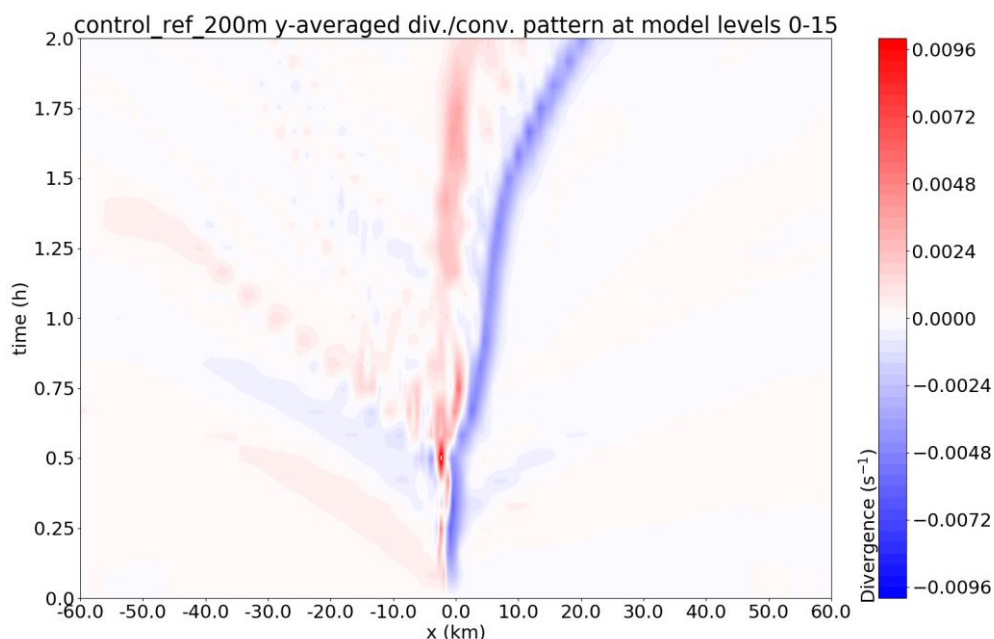


Figure S7a. Same as Figure 3a in main text, but without annotation.

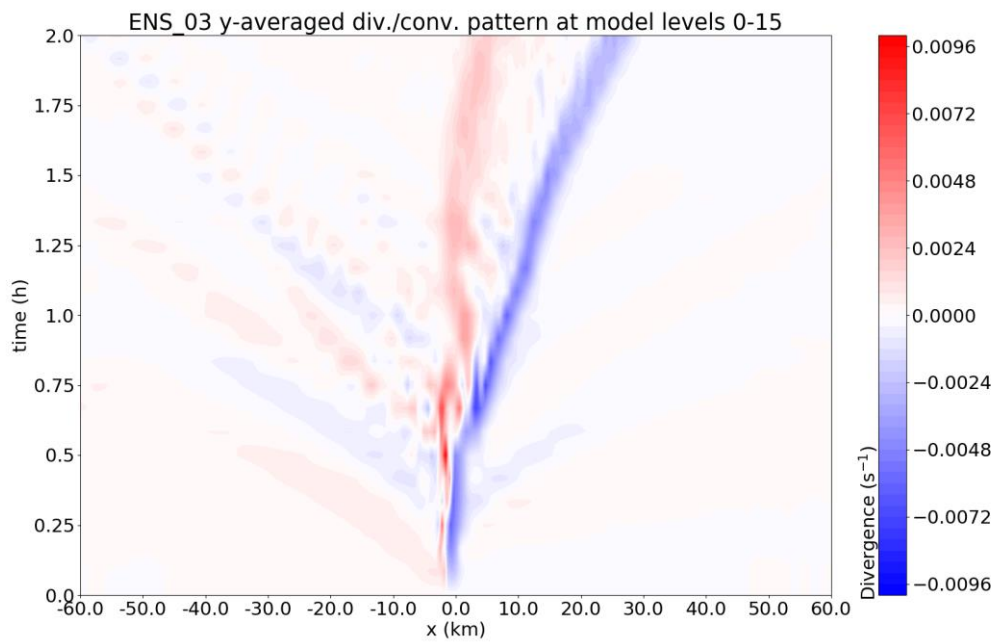


Figure 7b. Same as Figure 3b. in main text, but without annotations.

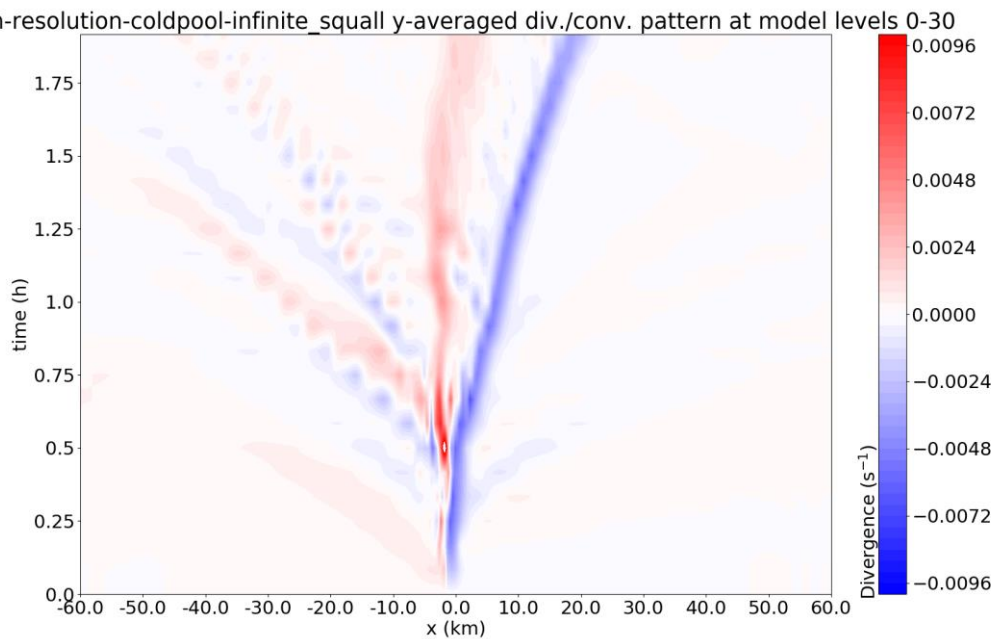


Figure 7c. Same, but for a simulation with 50 m vertical grid spacing.

Looking at figures S7a, S7b and S7c, the three evolutions differ only slightly and the third is an intermediate between the two. The cold pool is propagating by more than 10 km in ENS-03 over the interval 30-90 minutes, but by less than 10 km in the reference simulation. This corresponds with velocities of 2.5 m/s (9 km/h) and 4.3 m/s (15 km/h). In the high-resolution simulation, the propagation is about 11-12 km and it also initiates after 30 minutes. The way it initiates closely resembles the other two simulations: a strengthening of the convergence zone at $x = 0$ km, with subsequent double convergence branches after 35 minutes or so. The jump is comparatively very

pronounced in ENS-03 (especially in the divergence, less so in the convergence), subtle in the high-resolution simulation in especially the divergence (not in the convergence) and in practically absent – rather a smooth evolution – in the reference simulation.

This fits our expectations that increased resolution to resolve cold pool dynamics corresponds with an evolution within the ensemble envelope of the coarser resolution in terms of cold pool dynamics.

The difference in evolution between the ensemble envelope (as contained by ENS-03 and the reference) may arise in the last 20 or 30 minutes, with a pronounced acceleration in both ENS-03 and the reference, but a weaker acceleration in the high resolution simulation. This is beyond the scope of this study: the time window studied in detail is restricted to the first 80 minutes of simulations.

Time series ensemble sensitivity analysis – correlations and circulation anomalies

On the next pages the full time series of correlation and co-variance patterns obtained in the ensemble sensitivity analysis is available (see Figures 7 and 8 of the main text). First, the time series complementing Figure 7 is shown (correlation structure; Figure S8 series), followed by that complementing Figure 8 (u-amplitude; Figure S9 series). Then Figure 7 is repeated, but masked regions that are not significant at $\alpha = 0,05$ and restricted to the interval between 20 and 100 minutes of simulation time (Figure S10 series).

Early time evolution of ensemble sensitivity (in earlier version in the main text)

Initially, during the first 15 minutes of simulation time, the signals revealed by the ensemble sensitivity analysis contain very low amplitude patterns, that are virtually unnoticeable in terms of u-velocities associated with it. Based on their geometry and fast propagation speed, these waves have to be low frequency sound waves with wave lengths on the order of 5 km and can spontaneously develop from density anomalies. As the acoustic waves are from a practical perspective unrelated to the convection, their relationship with the squall line developments can be ignored.

After 15-20 minutes, the area within and in the immediate surroundings of the convective bubble, along the y-axis, shows some covariability with the source variable. Initially this signal is restricted to some of the middle troposphere and the immediate wake of the cold pool edge. The magnitude of the covariability is initially small, below 0.1 m/s, but very locally reaches 0.5-1 m/s by 20 minutes.

The somewhat turbulent signal has propagated vertically after 25 minutes and extends from the surface up to about $z = 12.5$ km, which corresponds with the region of developing cells. Its amplitude is now also noticeable in terms u-values: in the whole troposphere about 0.5 m/s. At this same instance, one see the first association of w_{loc} with an undulating wave signal travelling at the interface level z_i , as exposed by a trough and air that has sunk. That signal resembles a gravity wave, consistently with signals from the tracer analysis. None of the signals in the first 20-25 minutes pass the statistical robustness threshold: the amplitude may be considerable, but they are not systematically associated in a linear way with the source variable of the analysis.

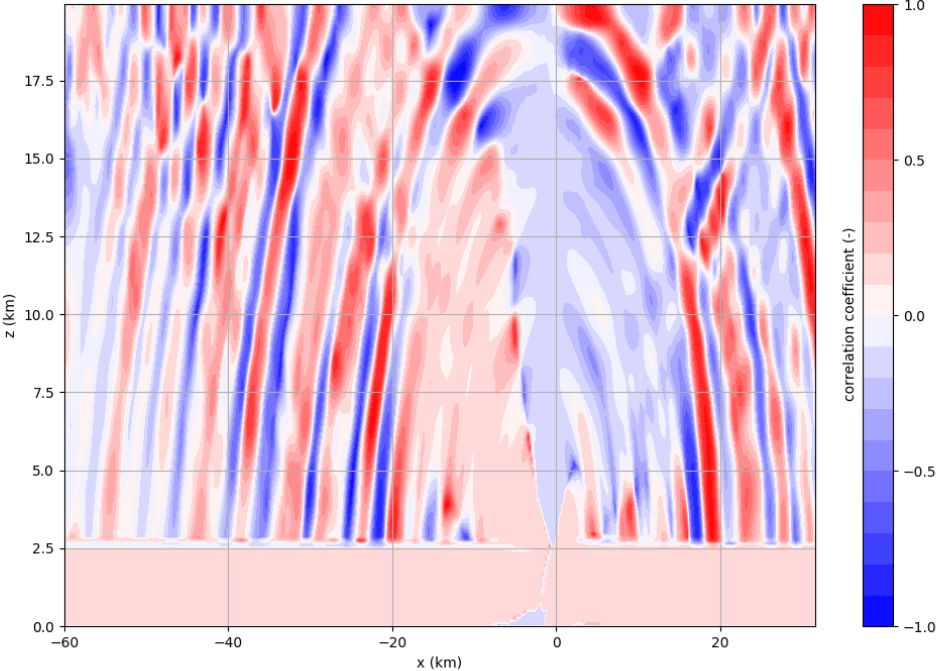
At the next time step, the former trough has propagated westward and the analysis is contained in the main paper text.

Late evolution of Ensemble Sensitivity

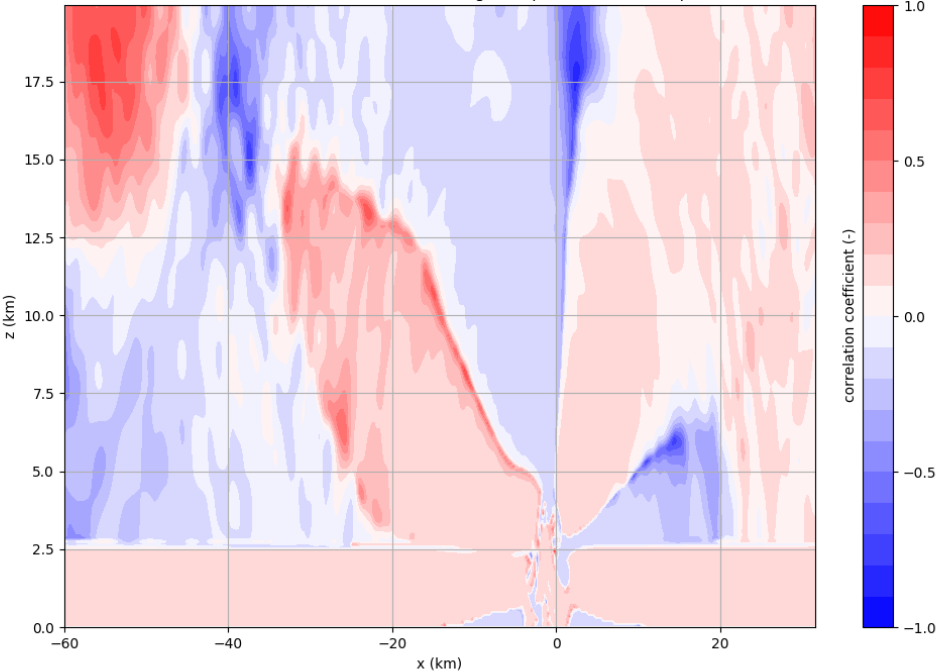
The anomalous flow pattern identified between 40 and 80 minutes is propagating away from its initiation region slowly while dying out. A new stage of variability manifests, with opposite signs but smaller amplitude coming in place of the earlier pattern.

Figure S8 series:

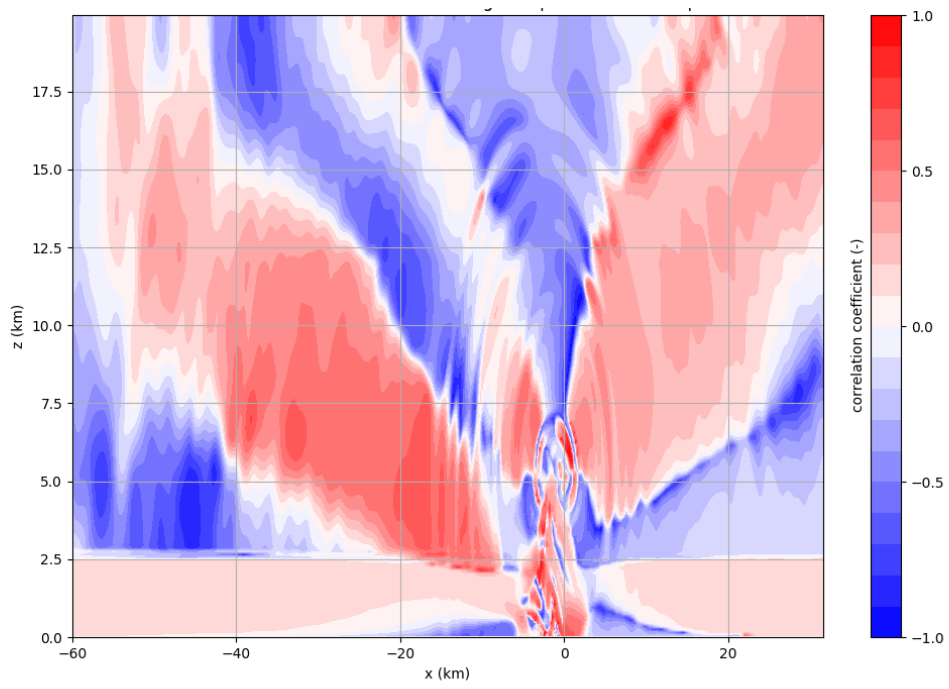
5 min:



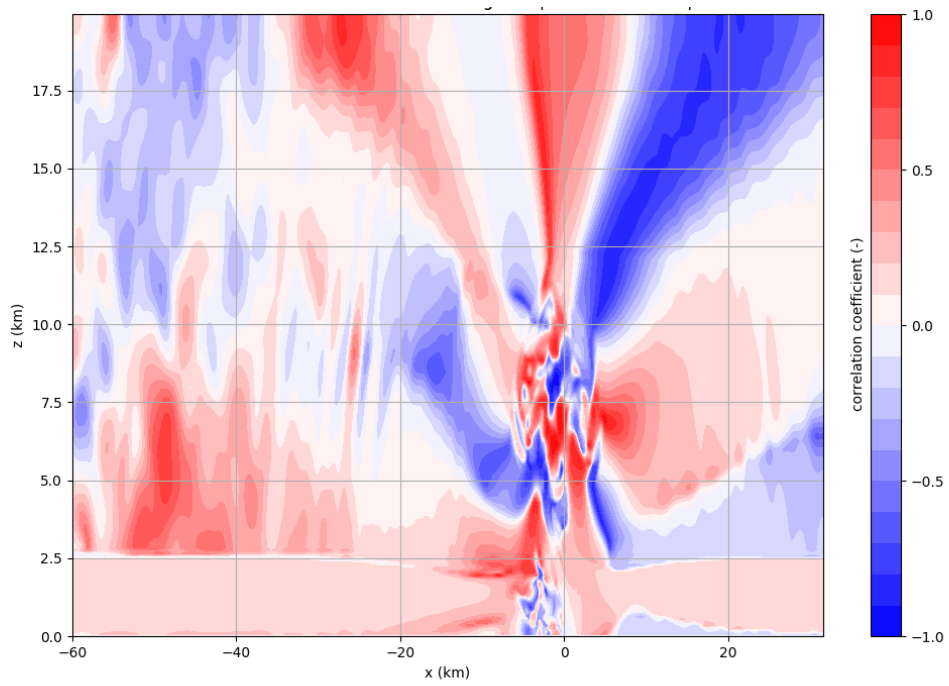
10 min:



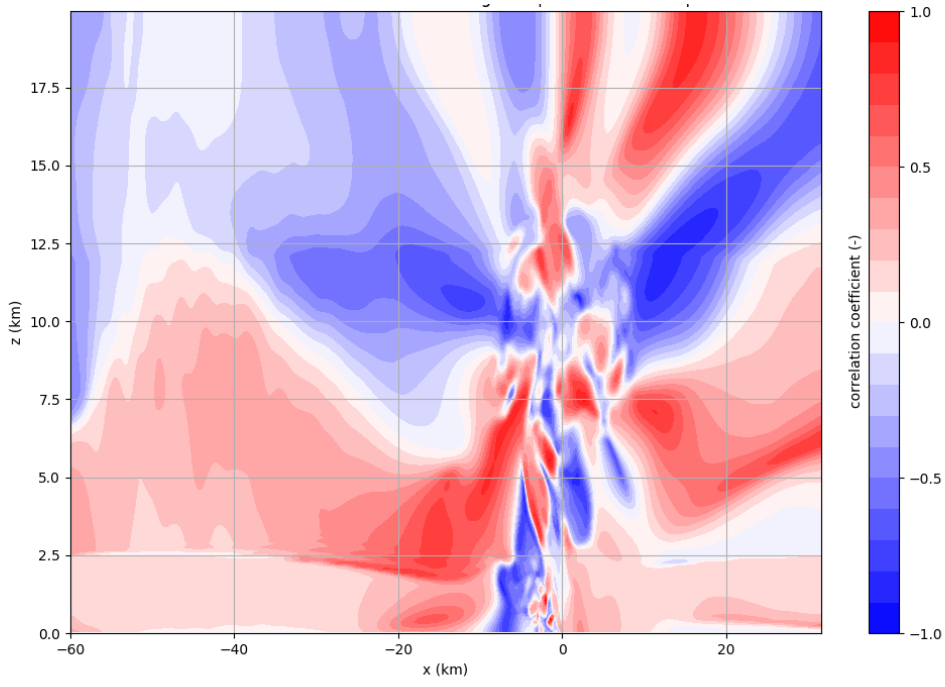
15 min:



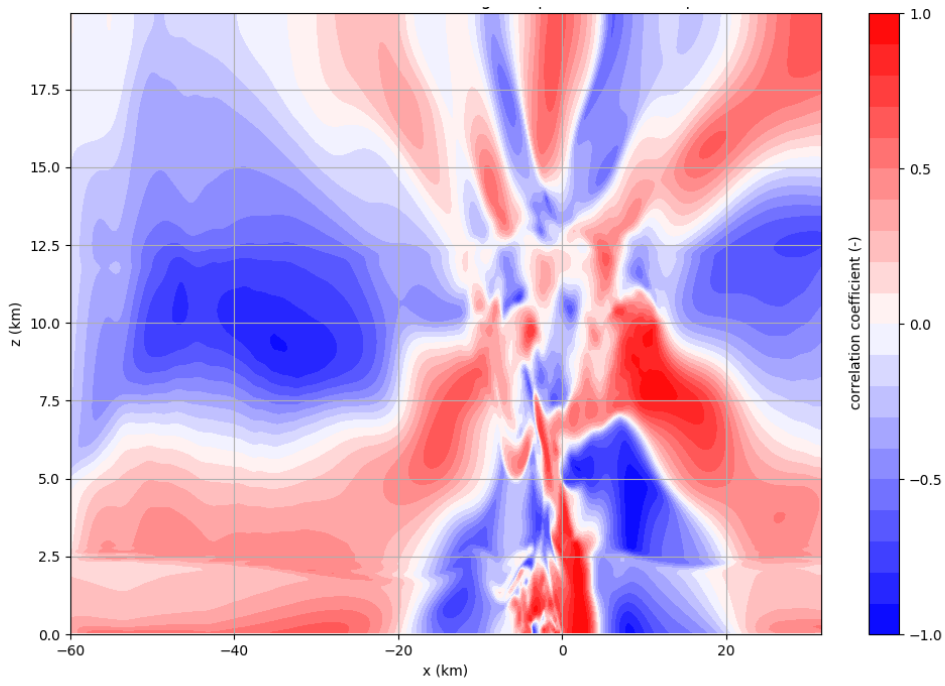
20 min:



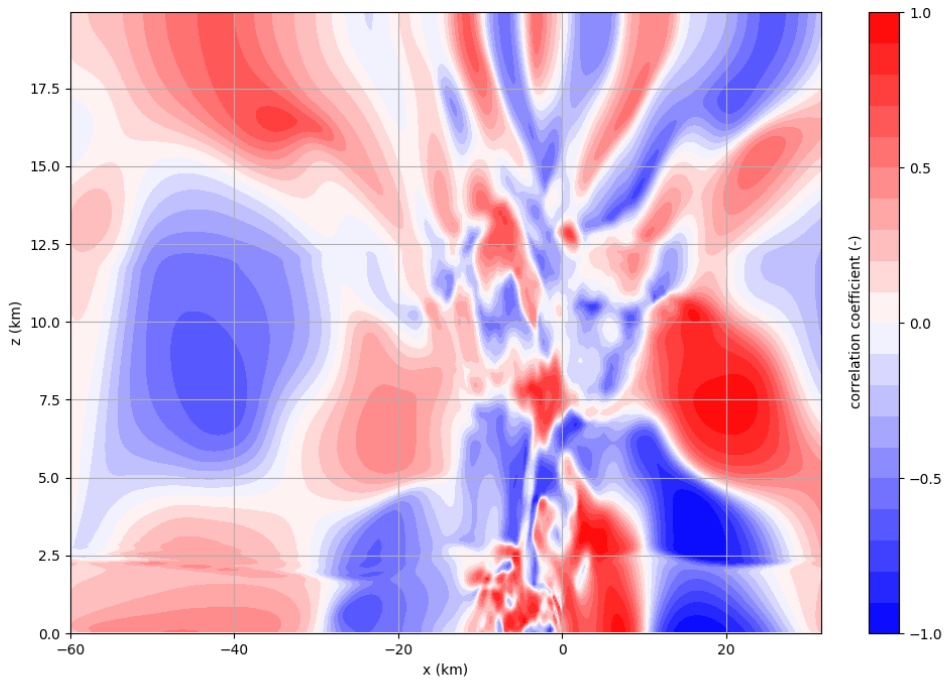
25 min:



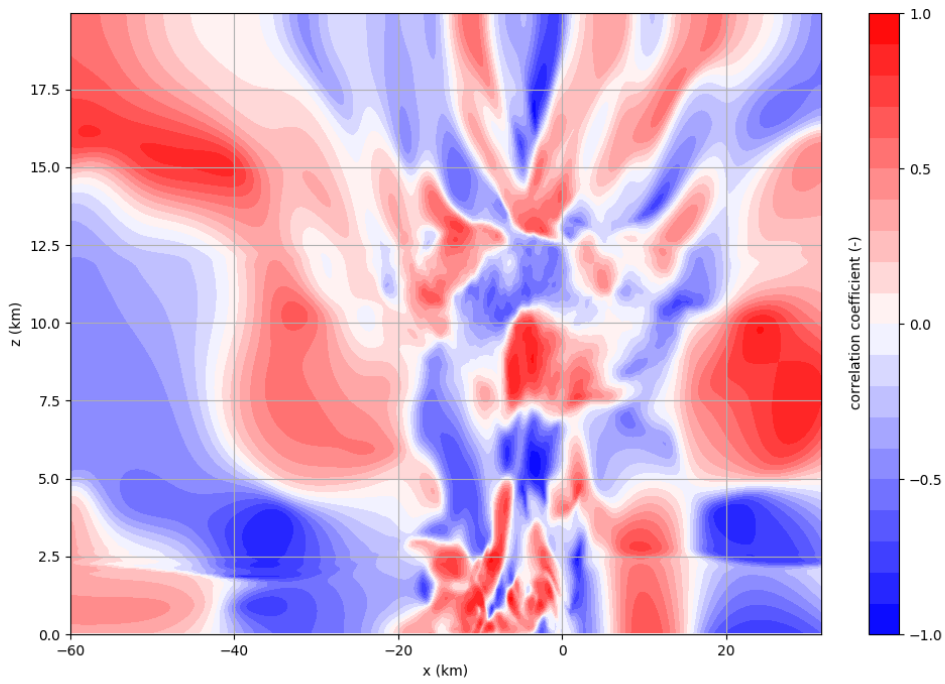
30 min:



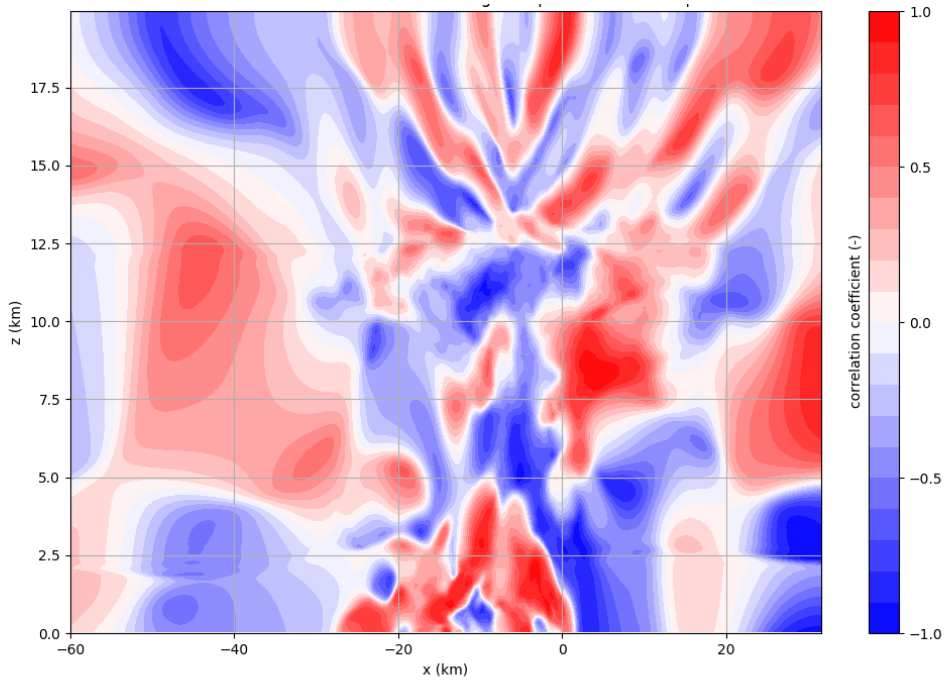
35 min:



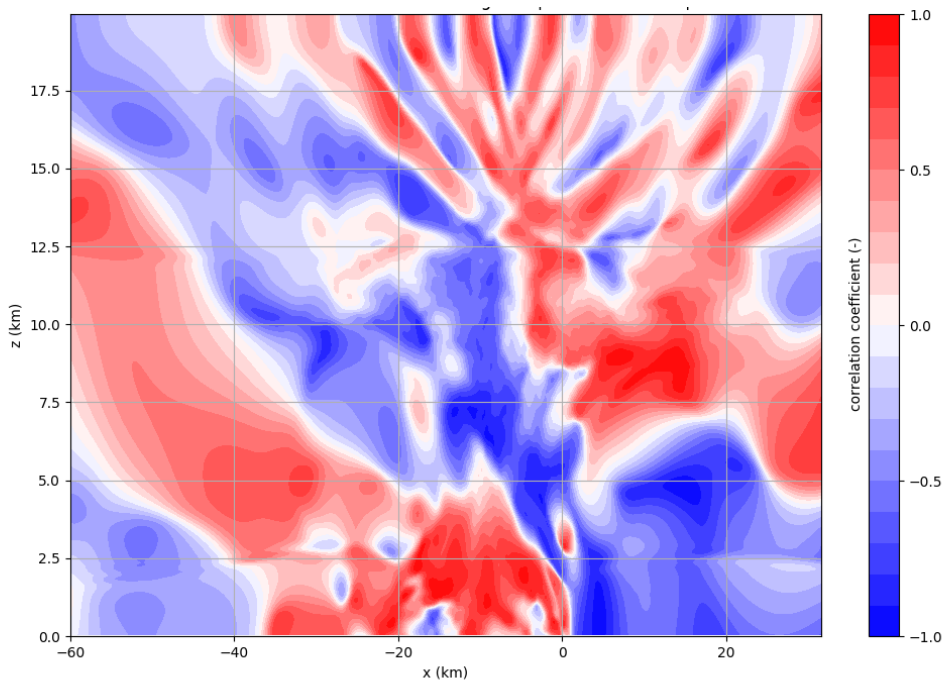
40 min:



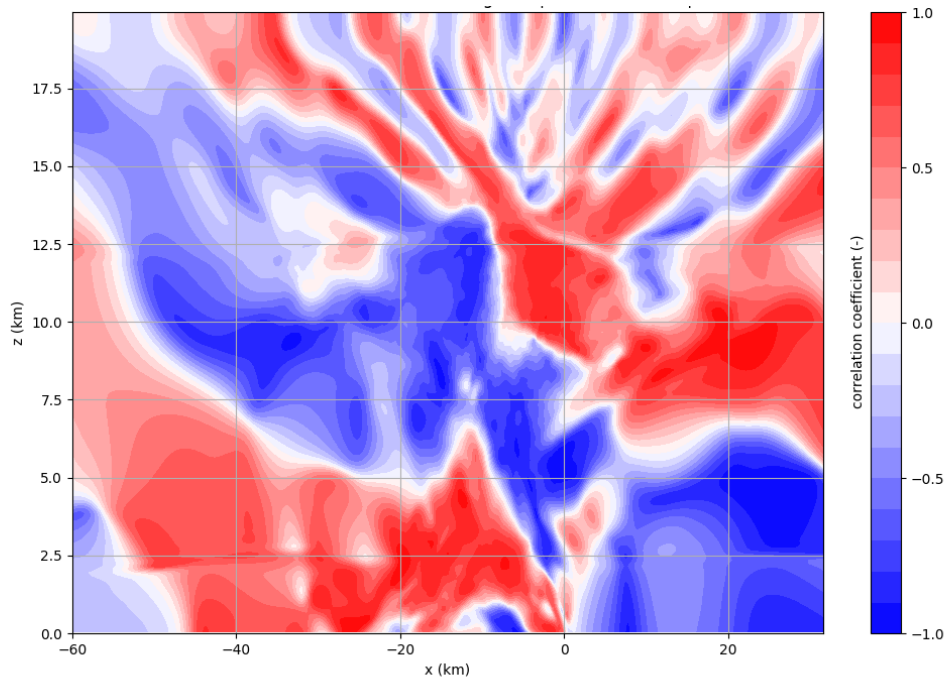
45 min:



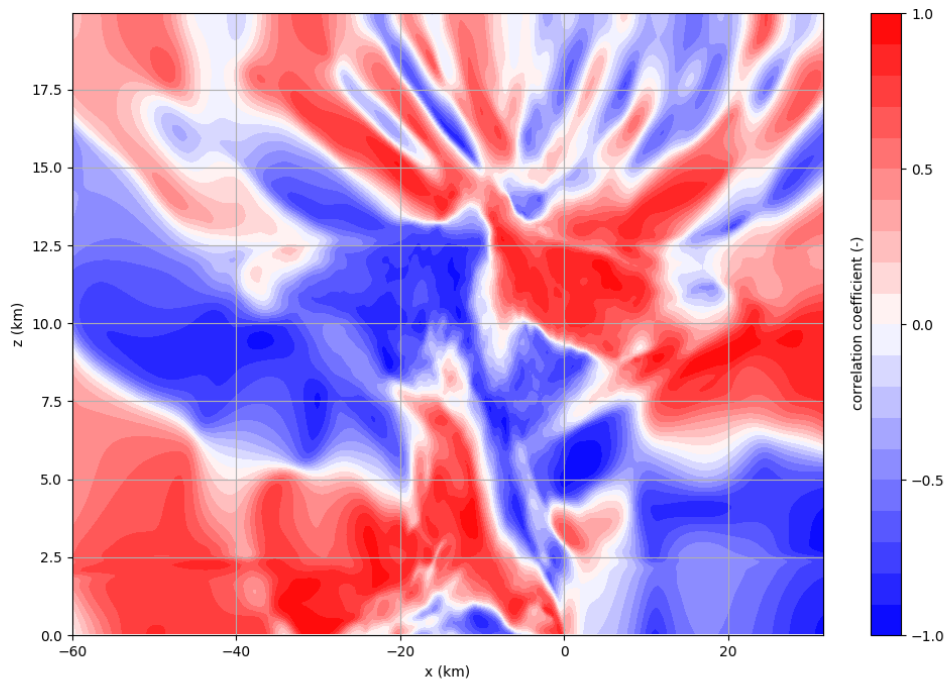
50 min:



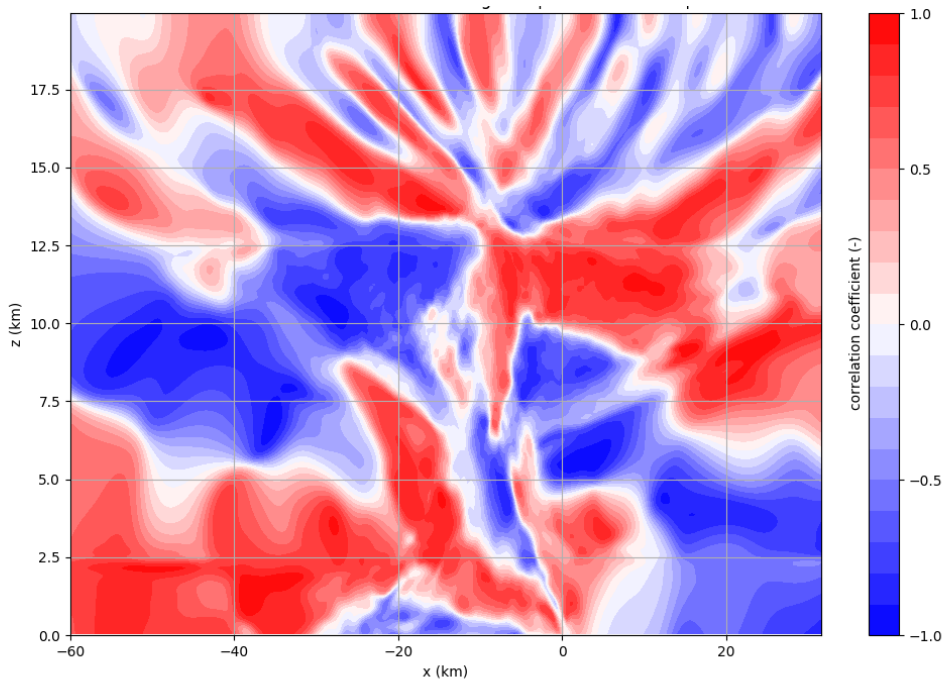
55 min:



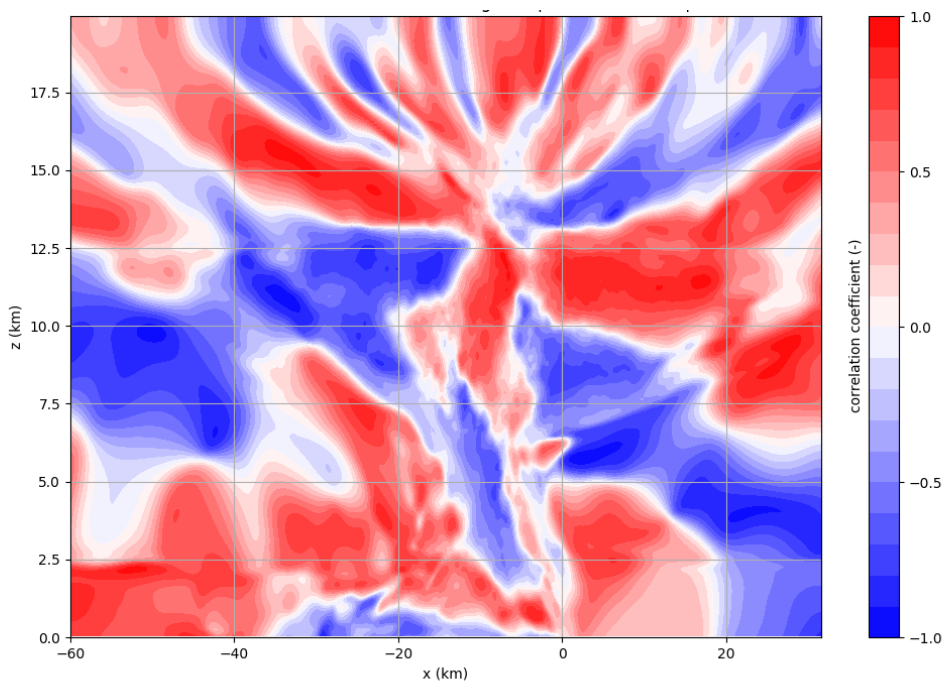
60 min:



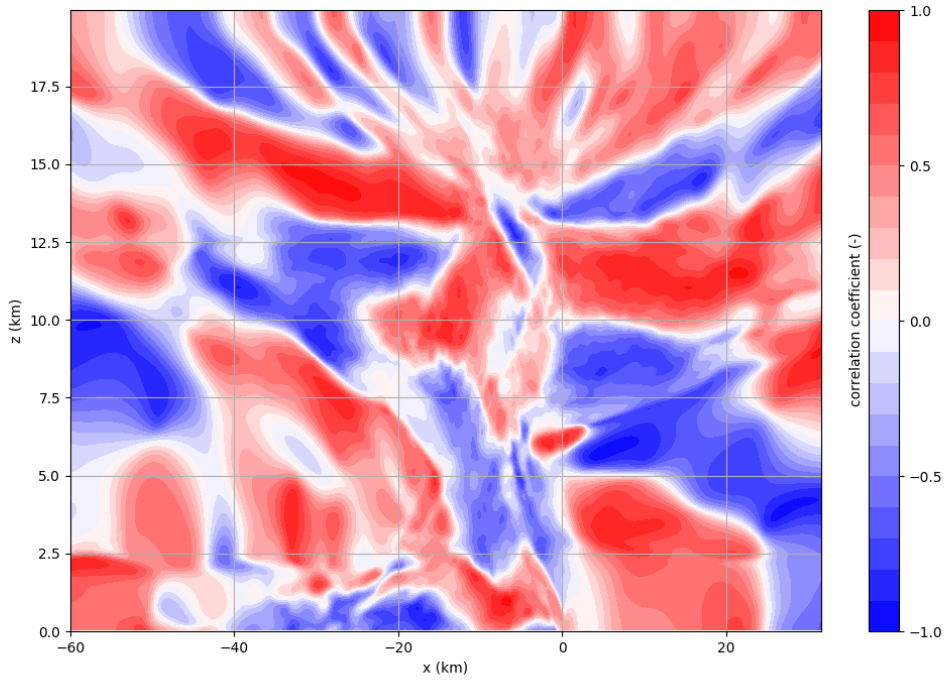
65 min:



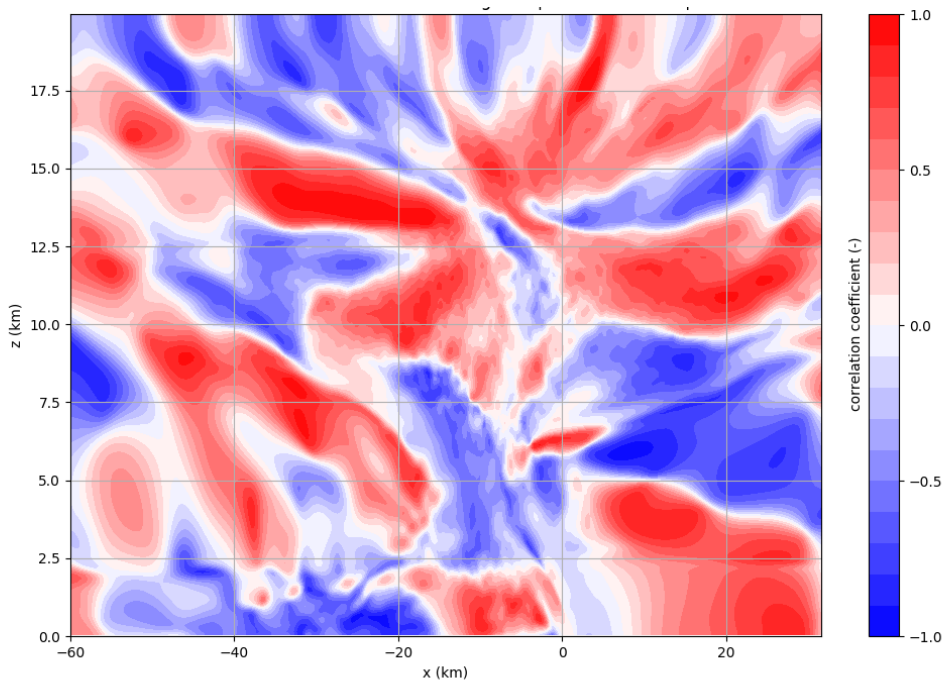
70 min:



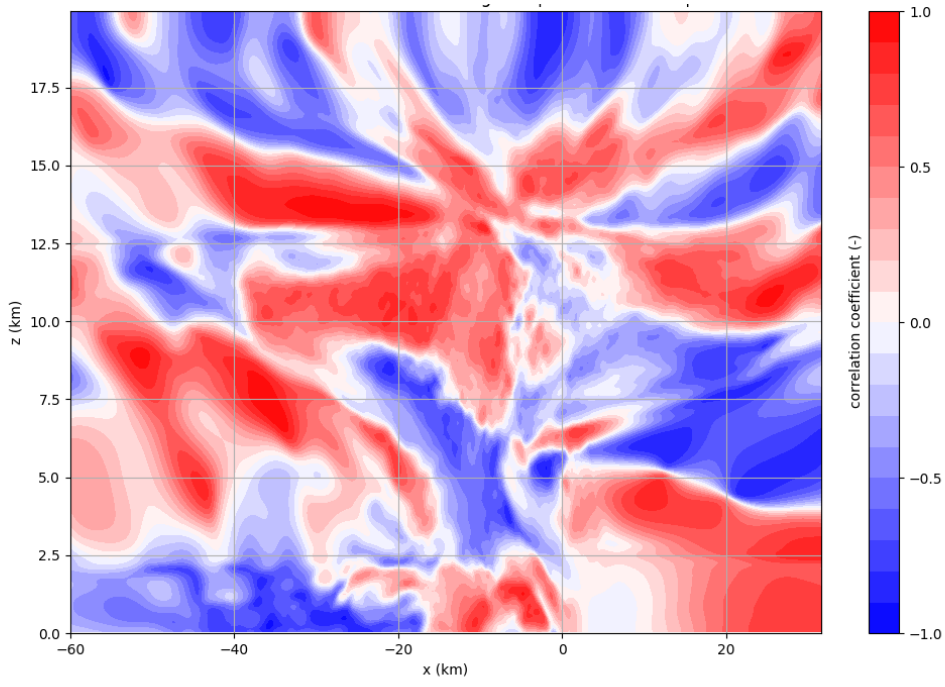
75 min:



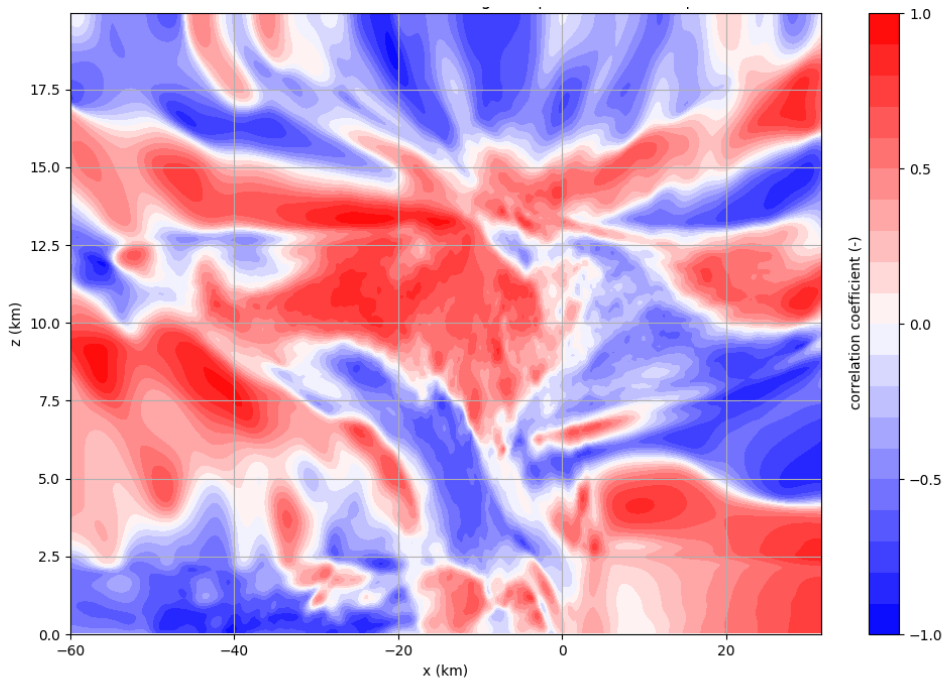
80 min:



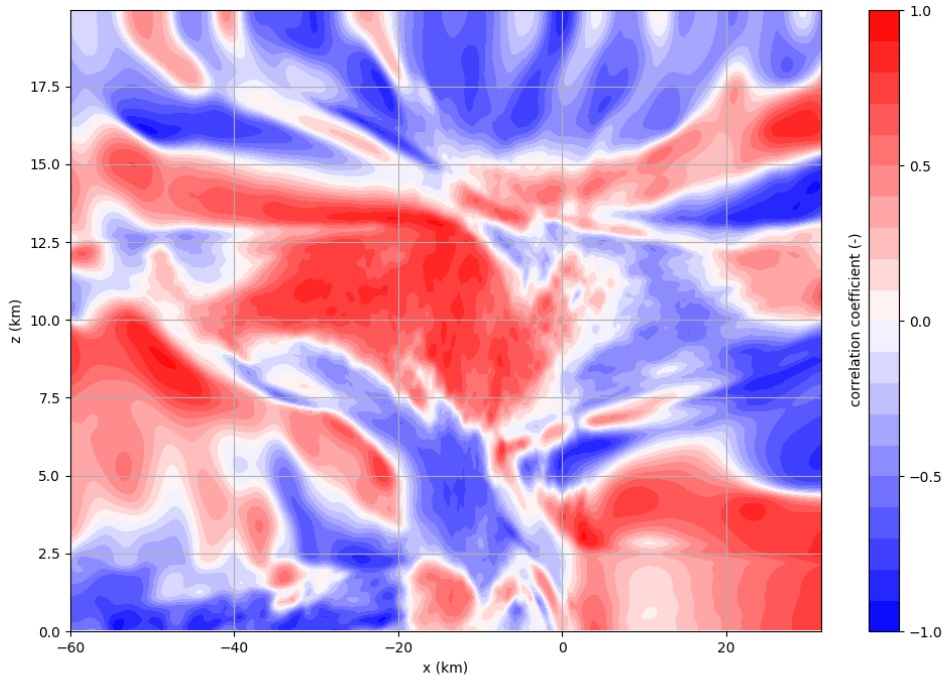
85 min:



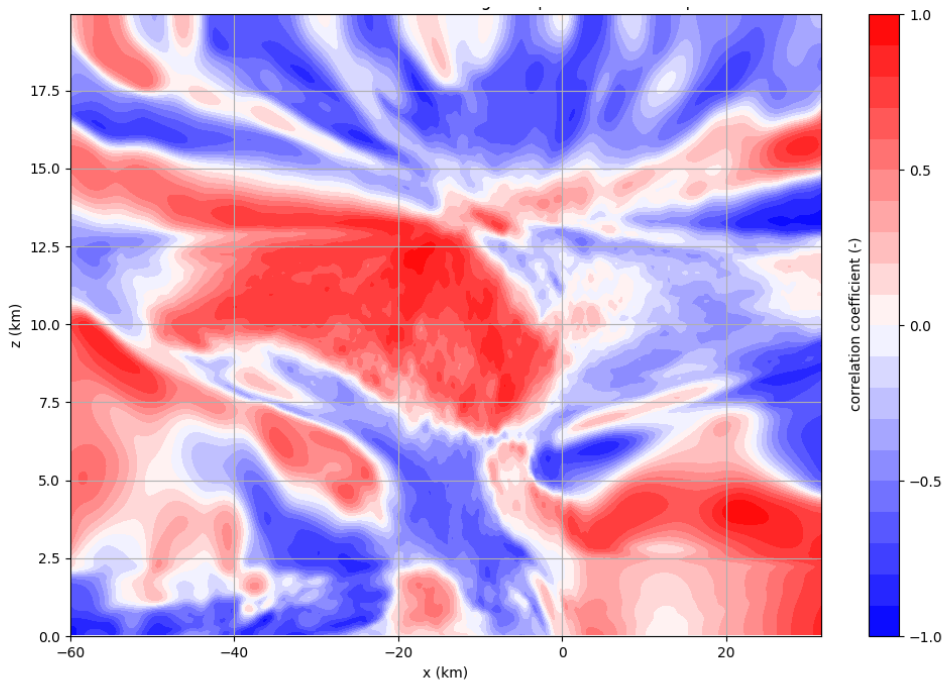
90 min:



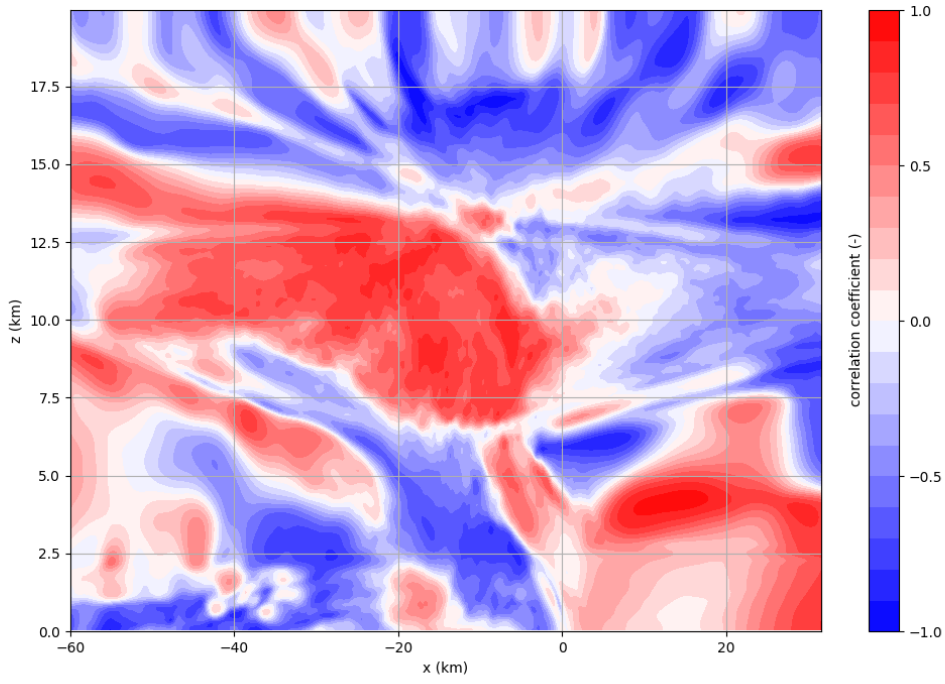
95 min:



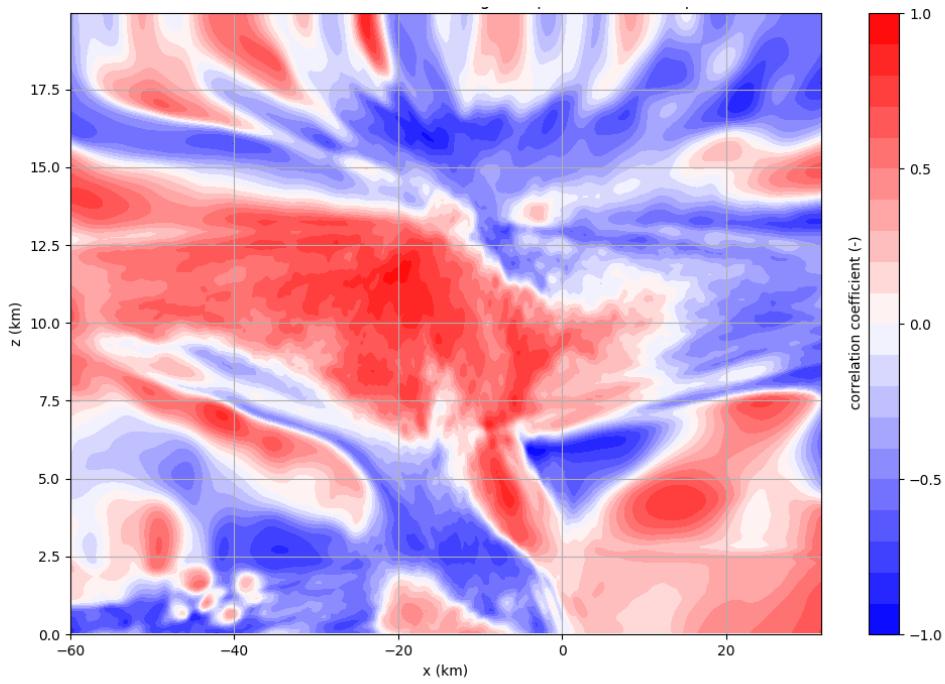
100 min:



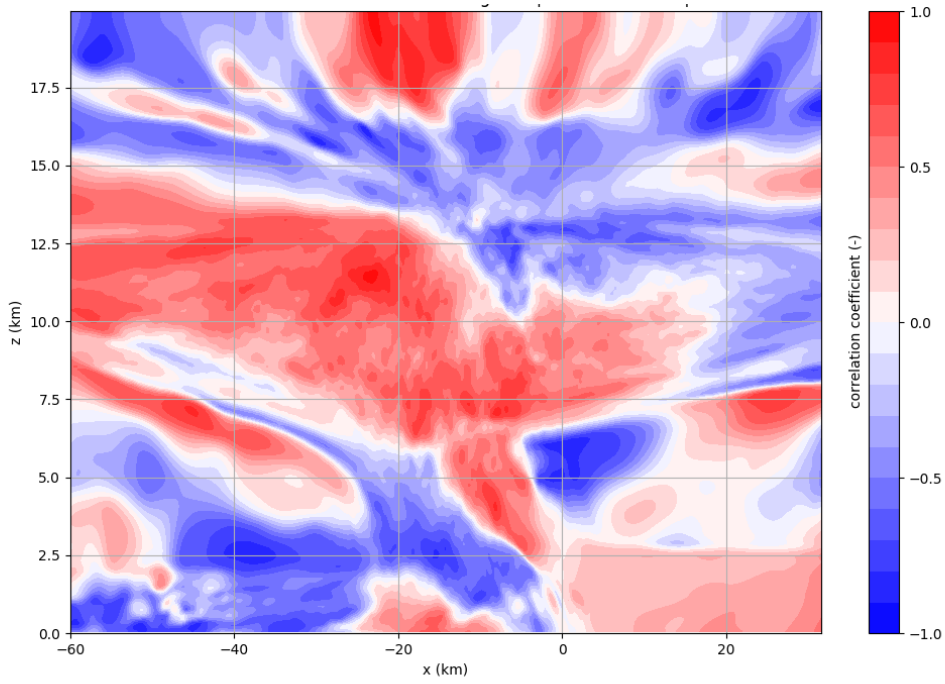
105 min:



110 min:



115 min:



120 min:

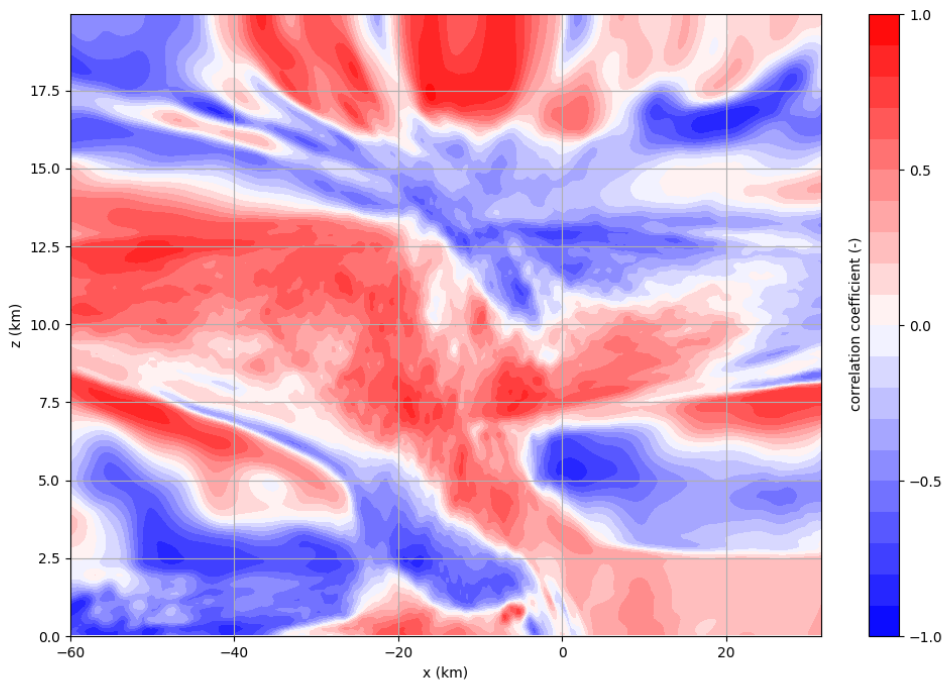
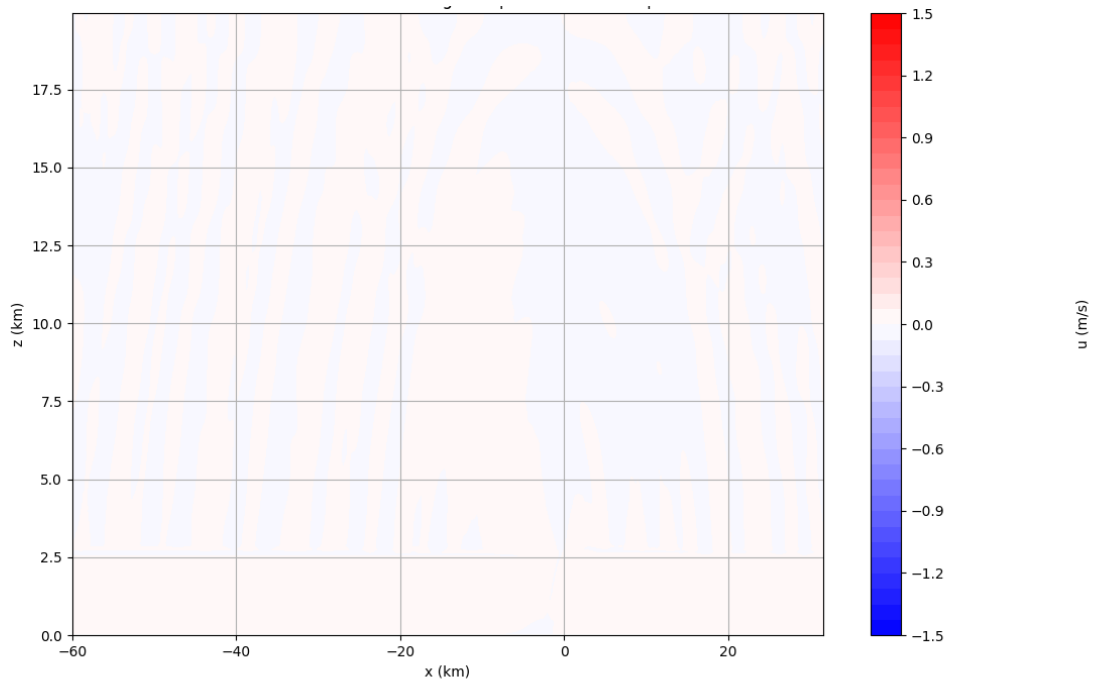
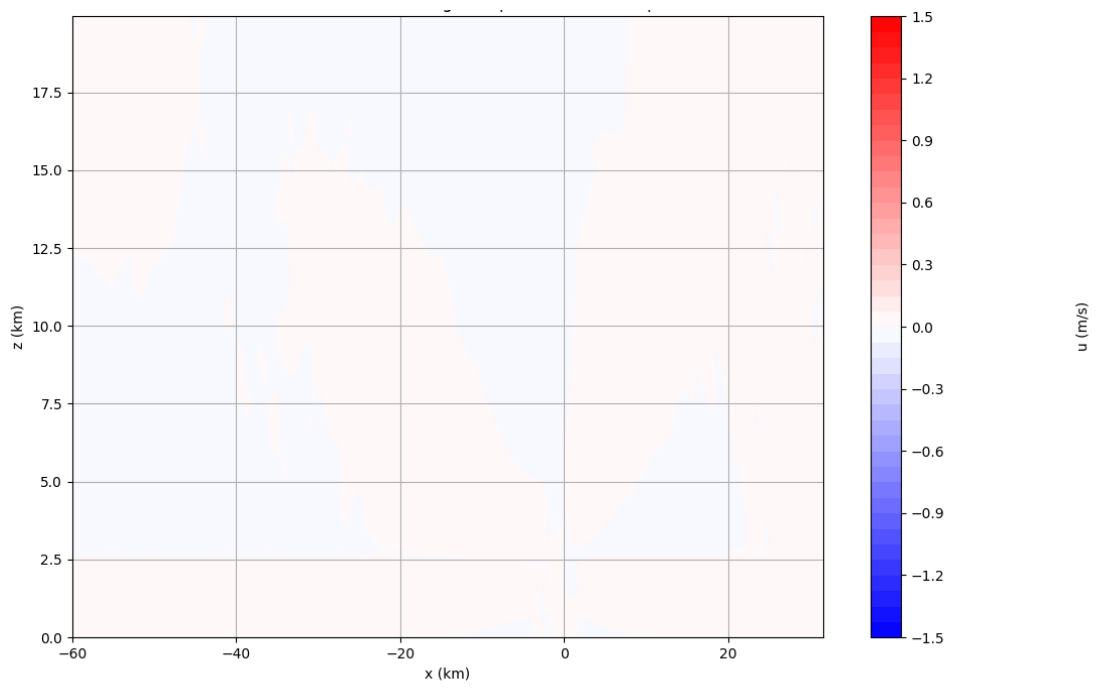


Figure S9 series: U-amplitude of co-variance/anomaly

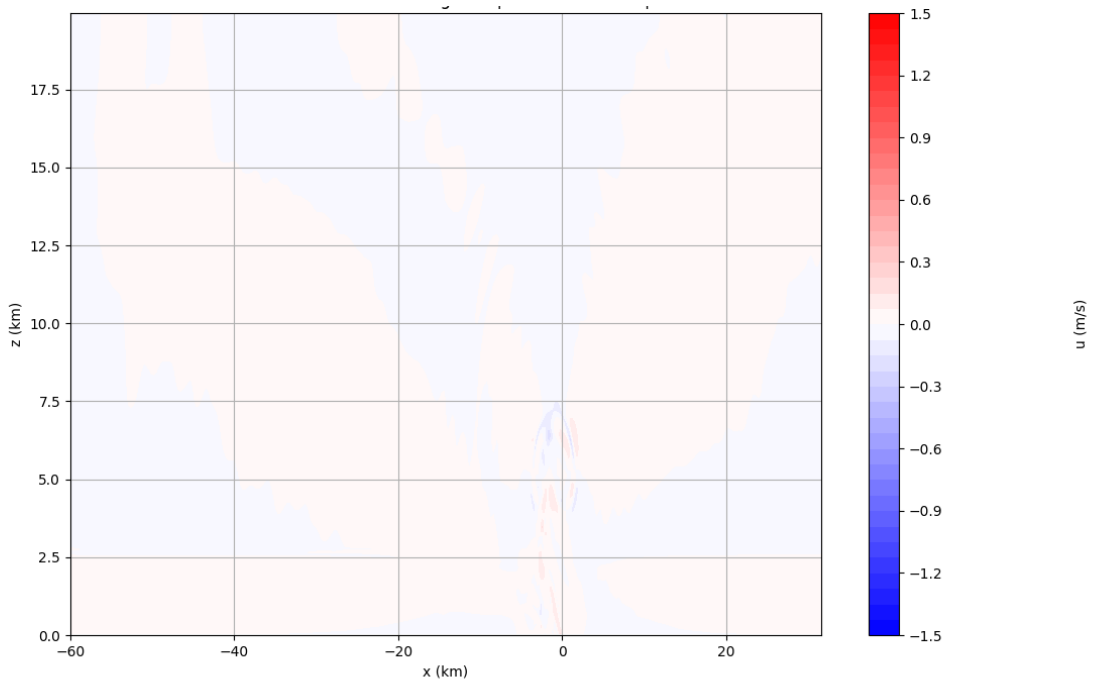
5 min:



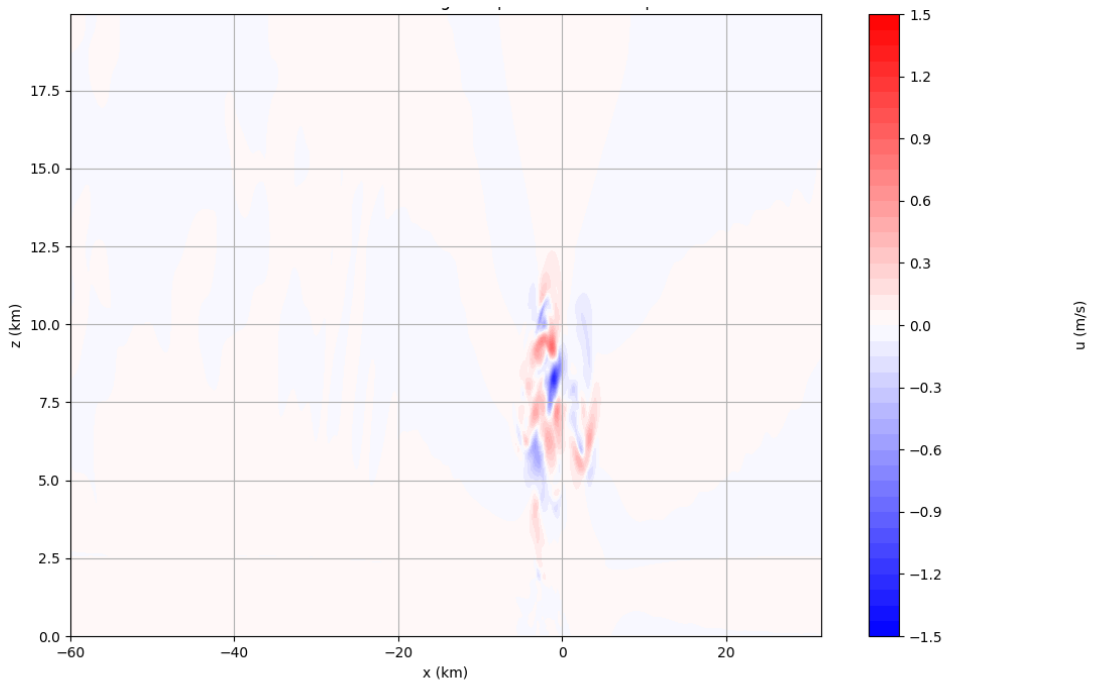
10 min:



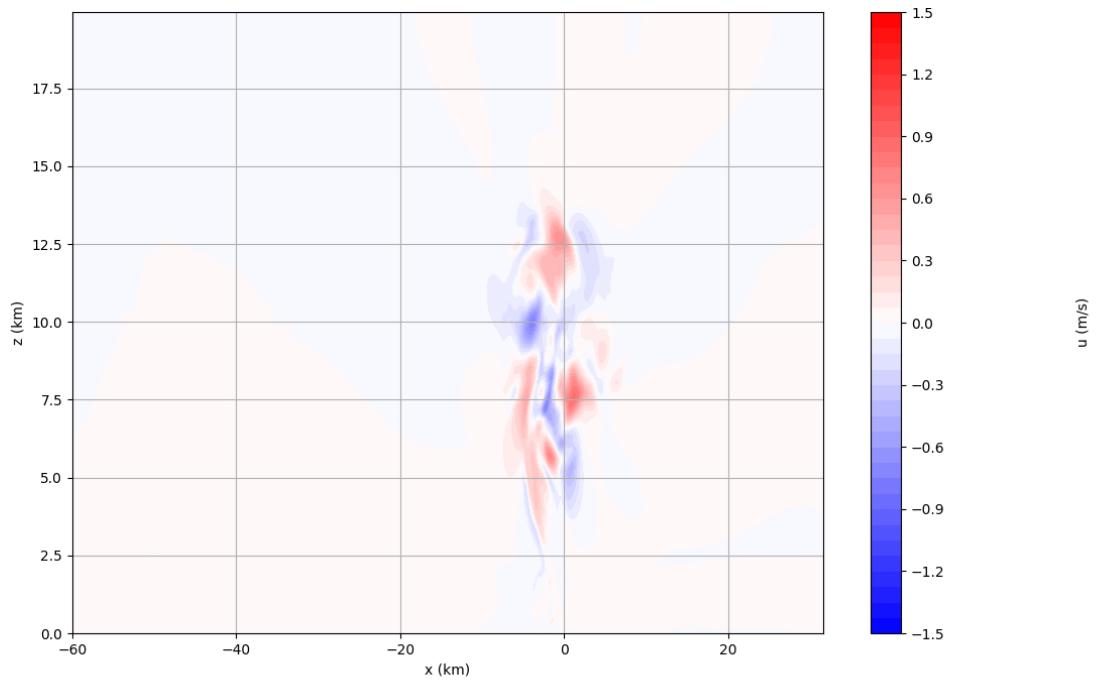
15 min:



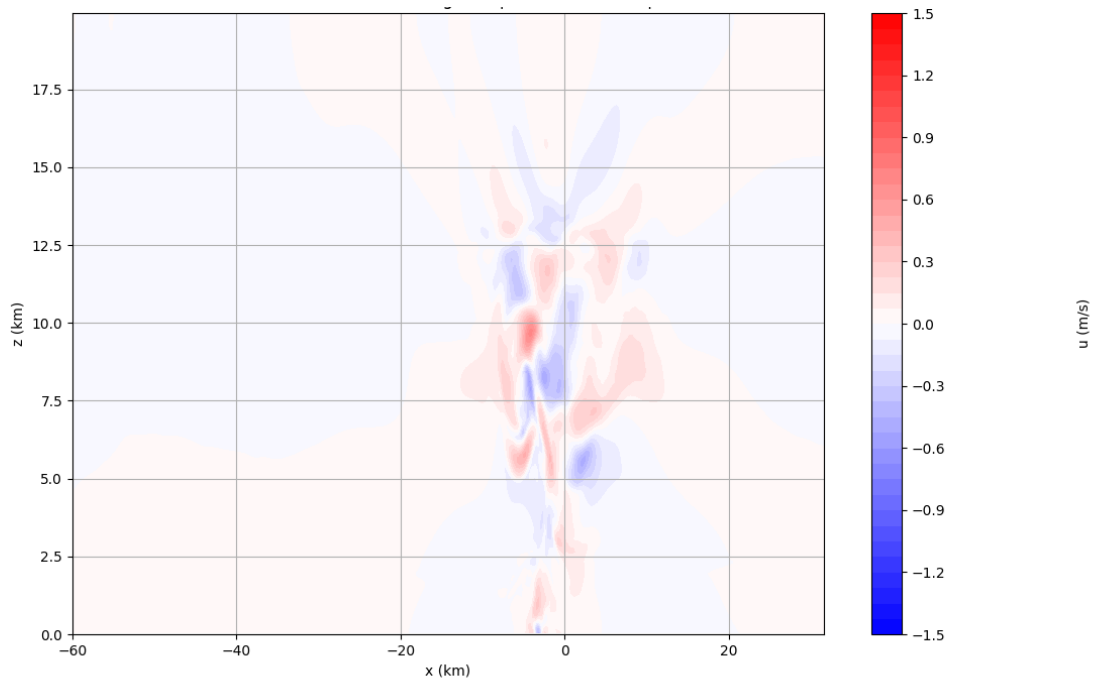
20 min:



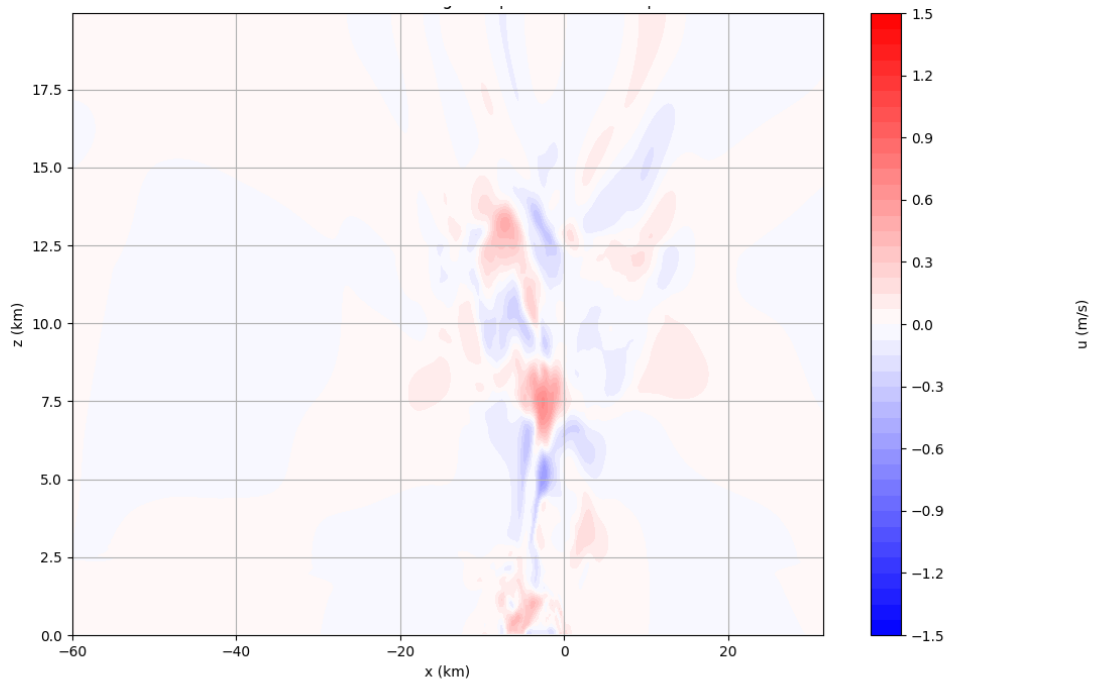
25 min:



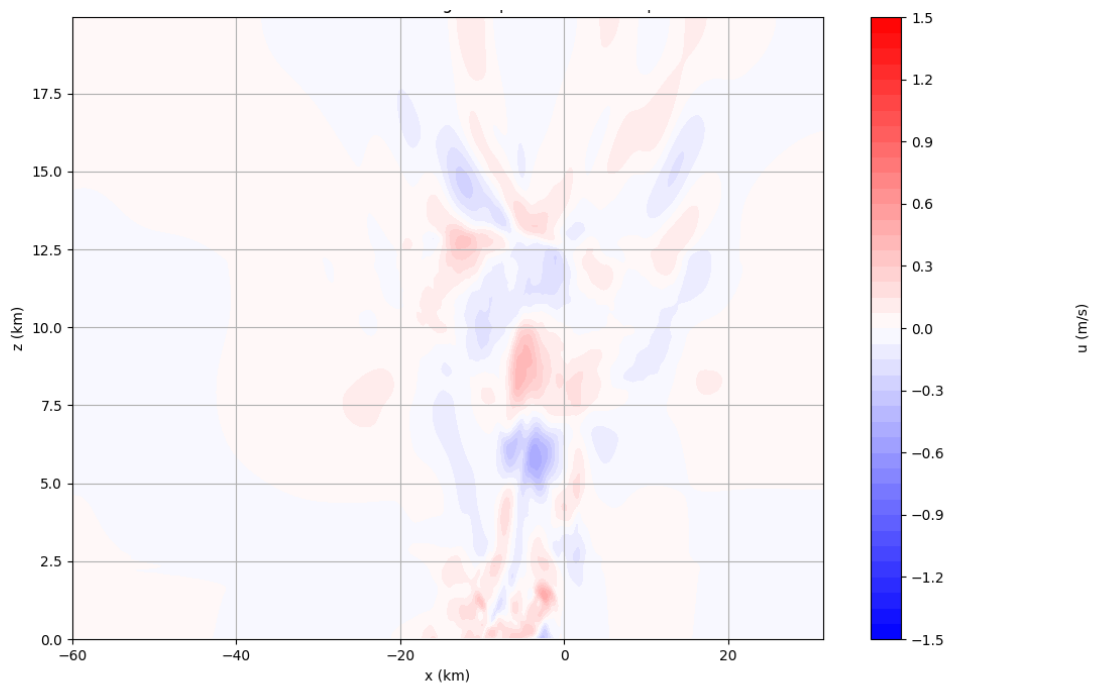
30 min:



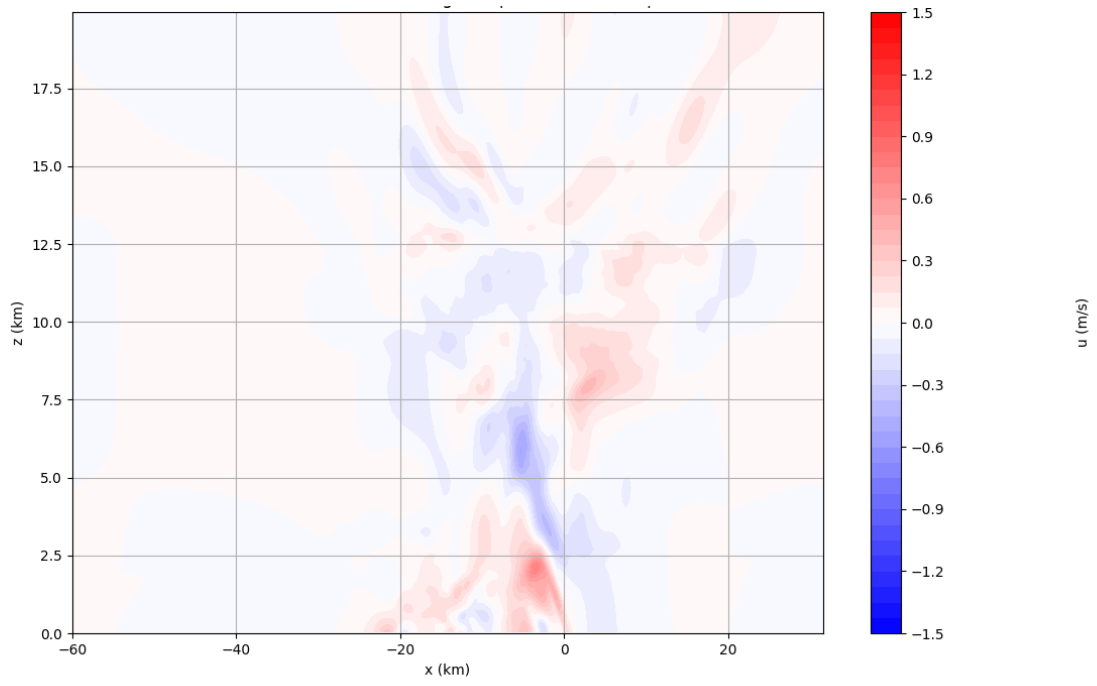
35 min:



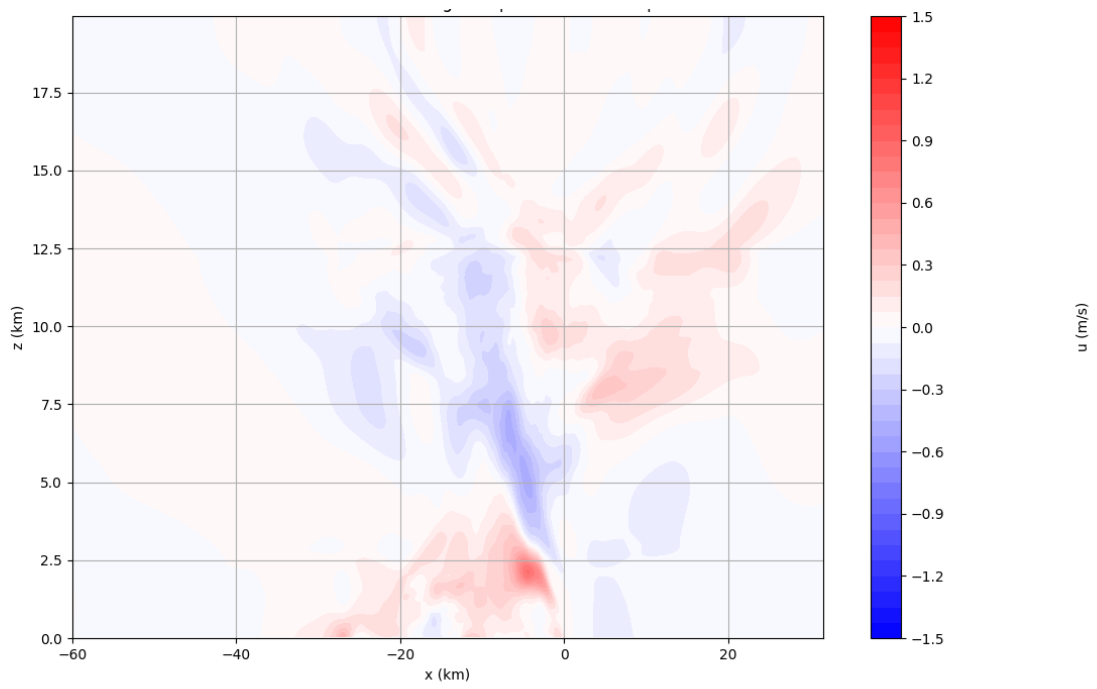
40 min:



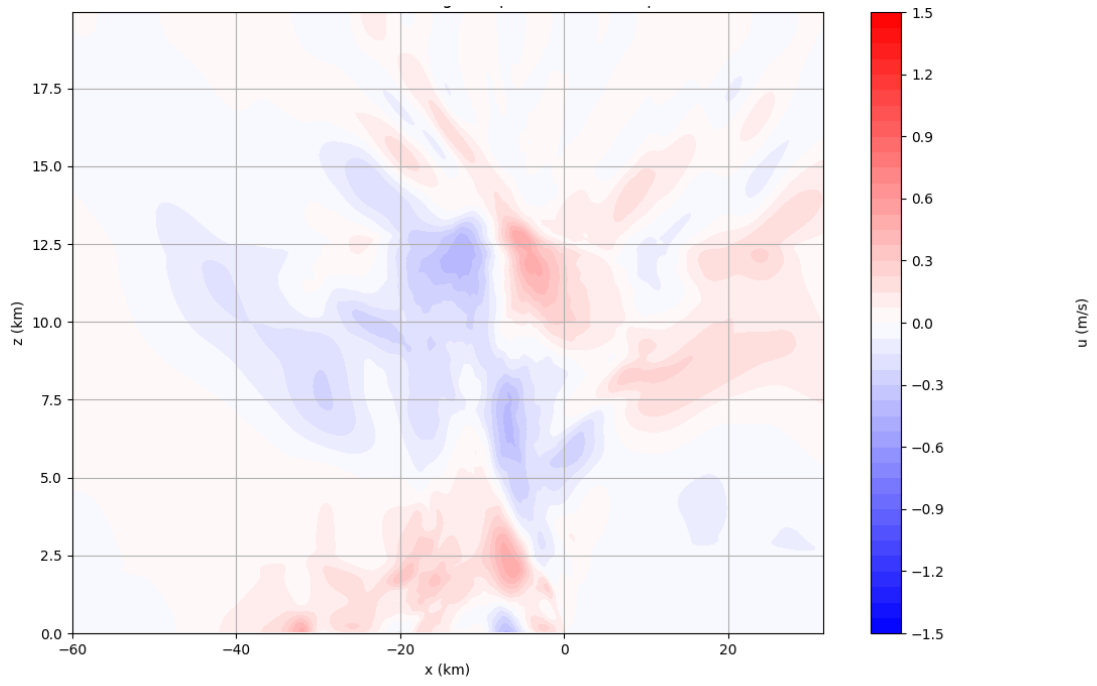
45 min:



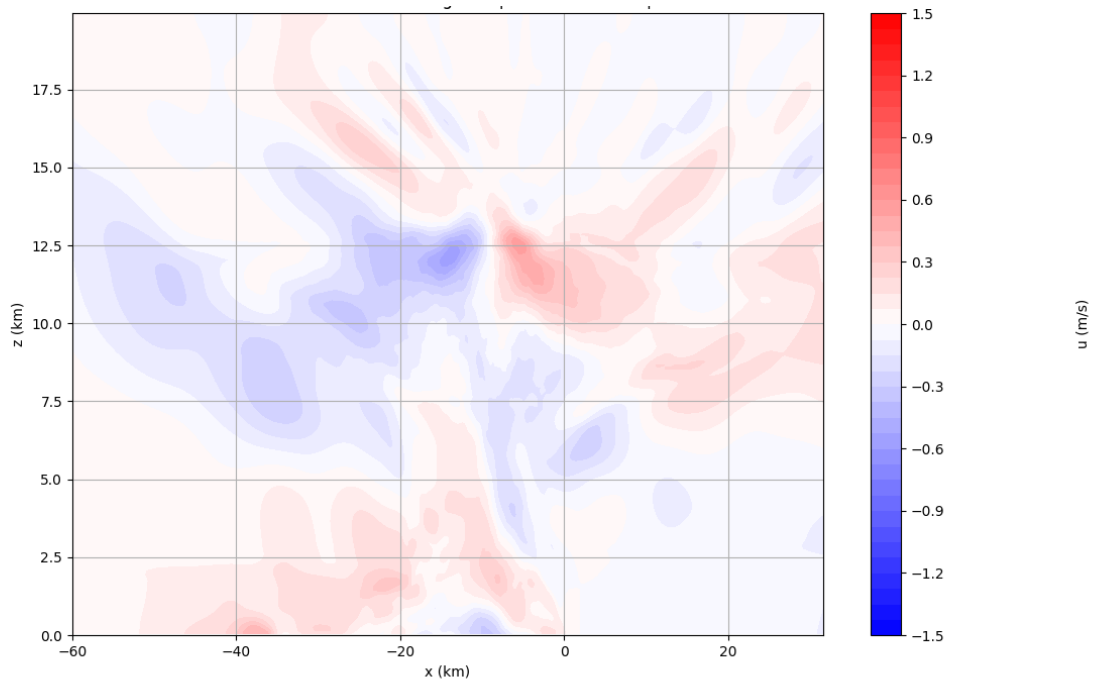
50 min:



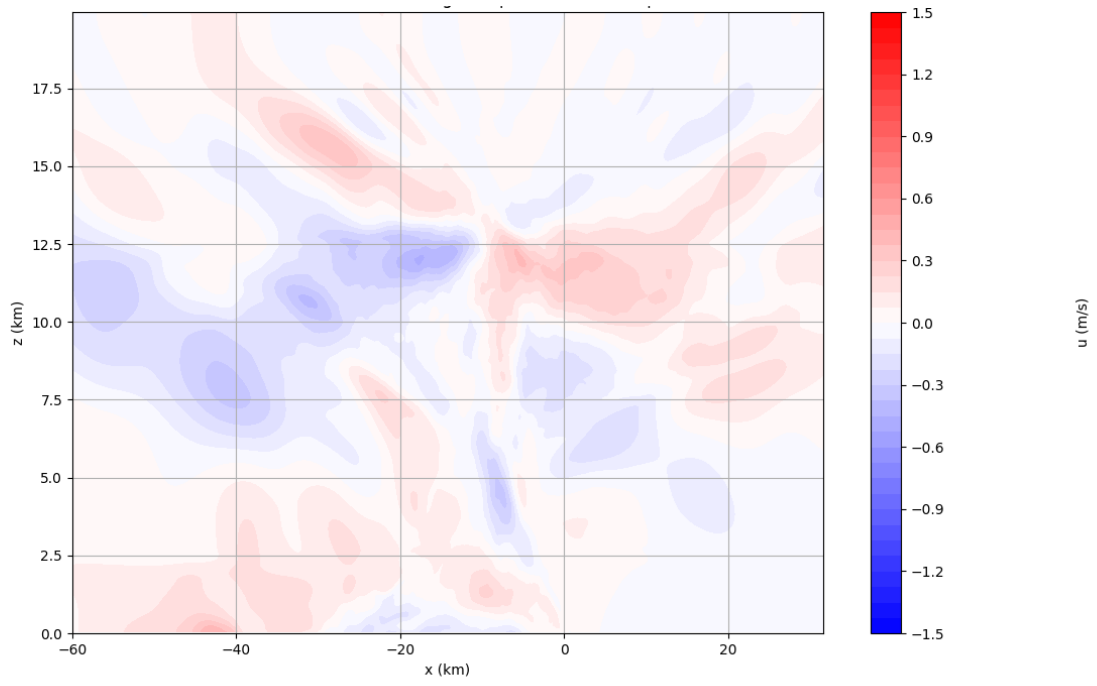
55 min:



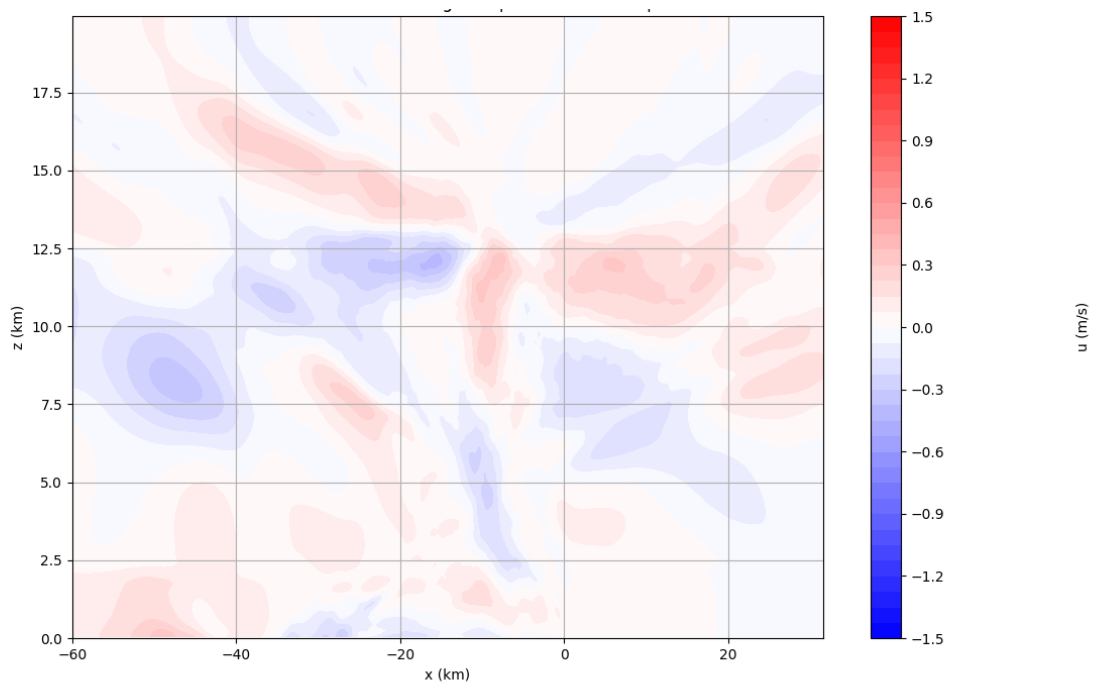
60 min:



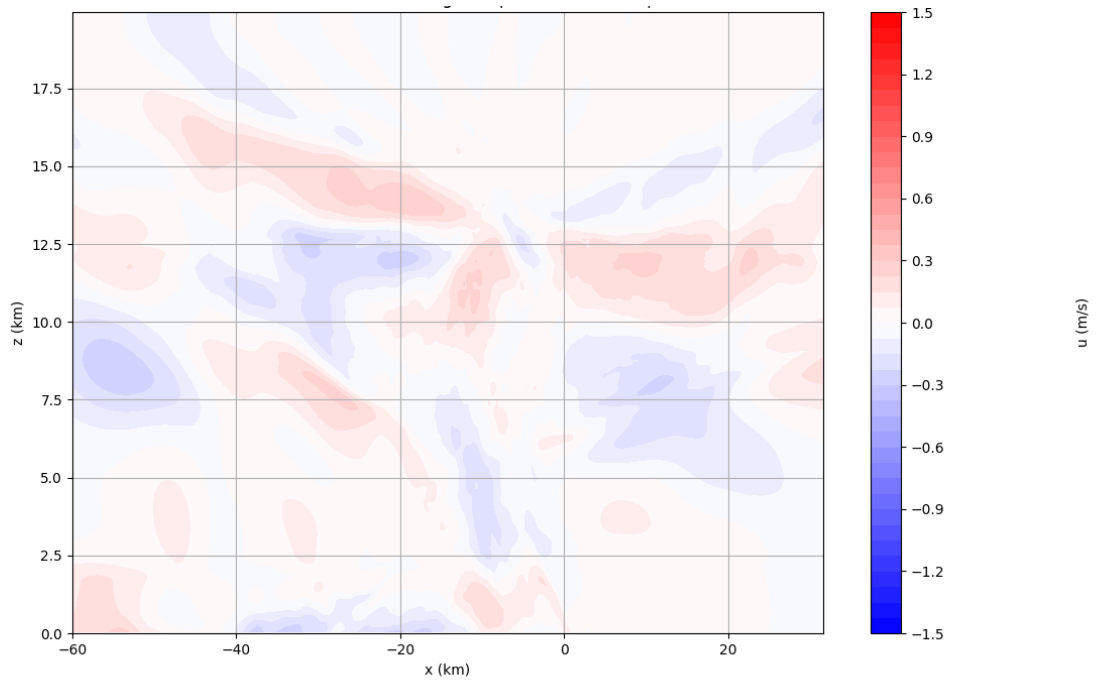
65 min:



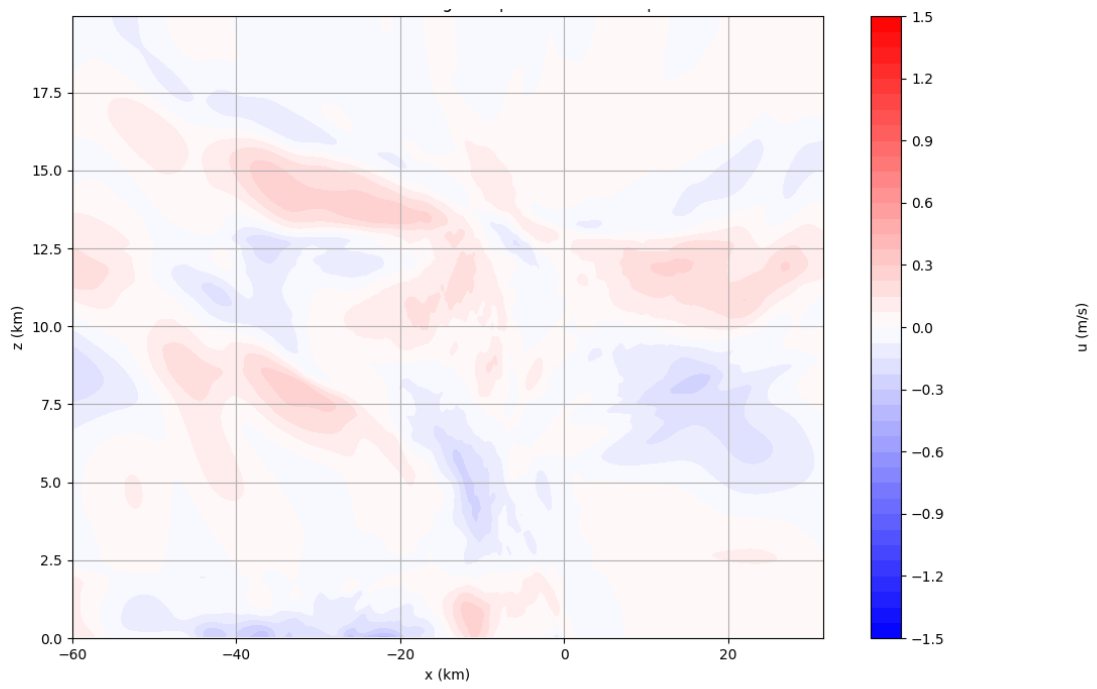
70 min:



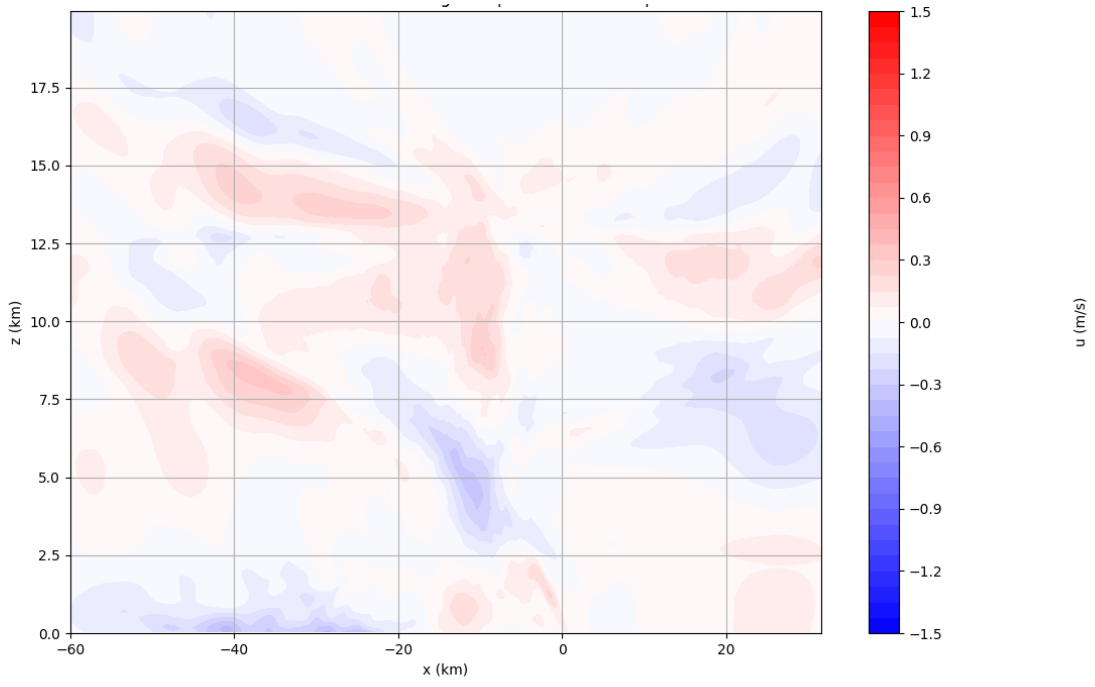
75 min:



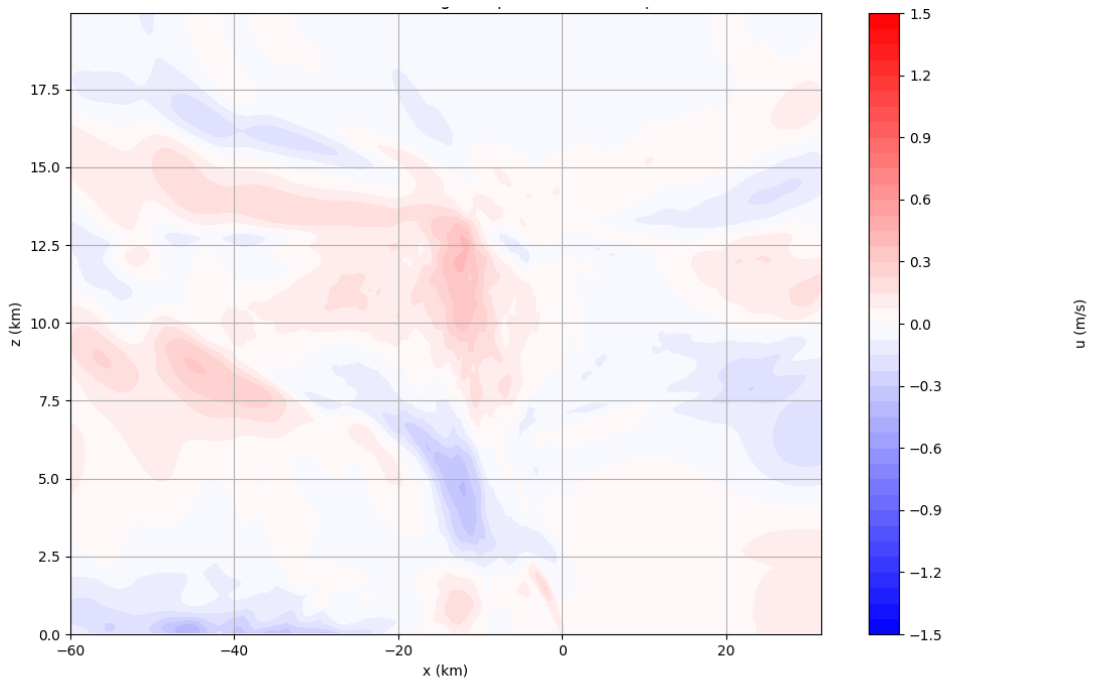
80 min:



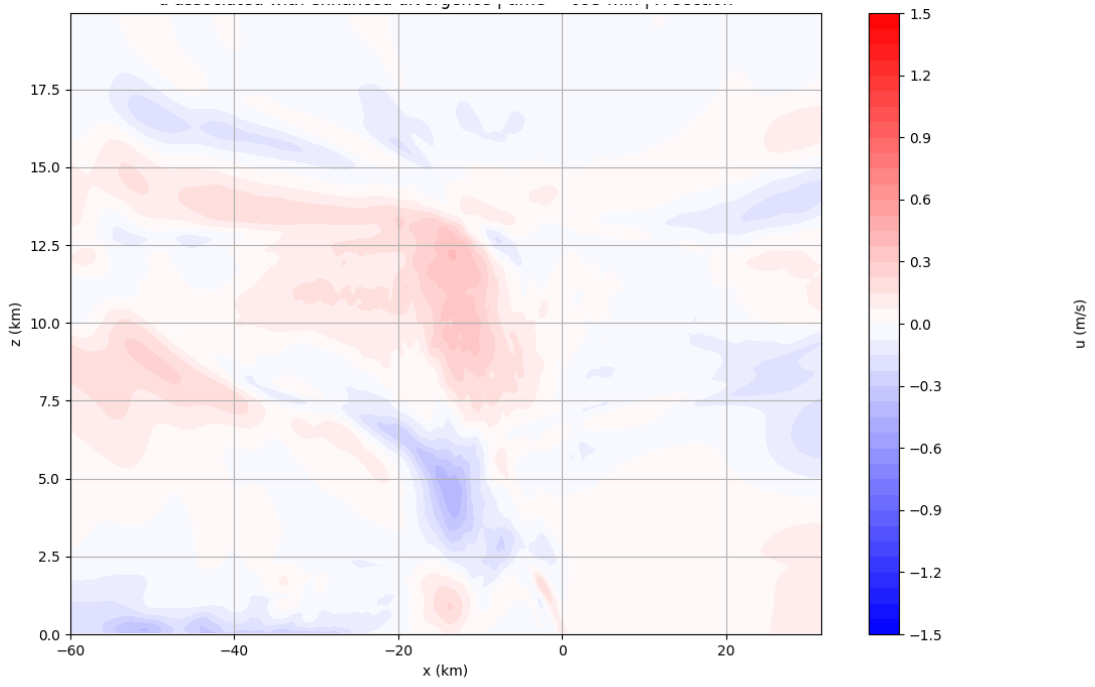
85 min:



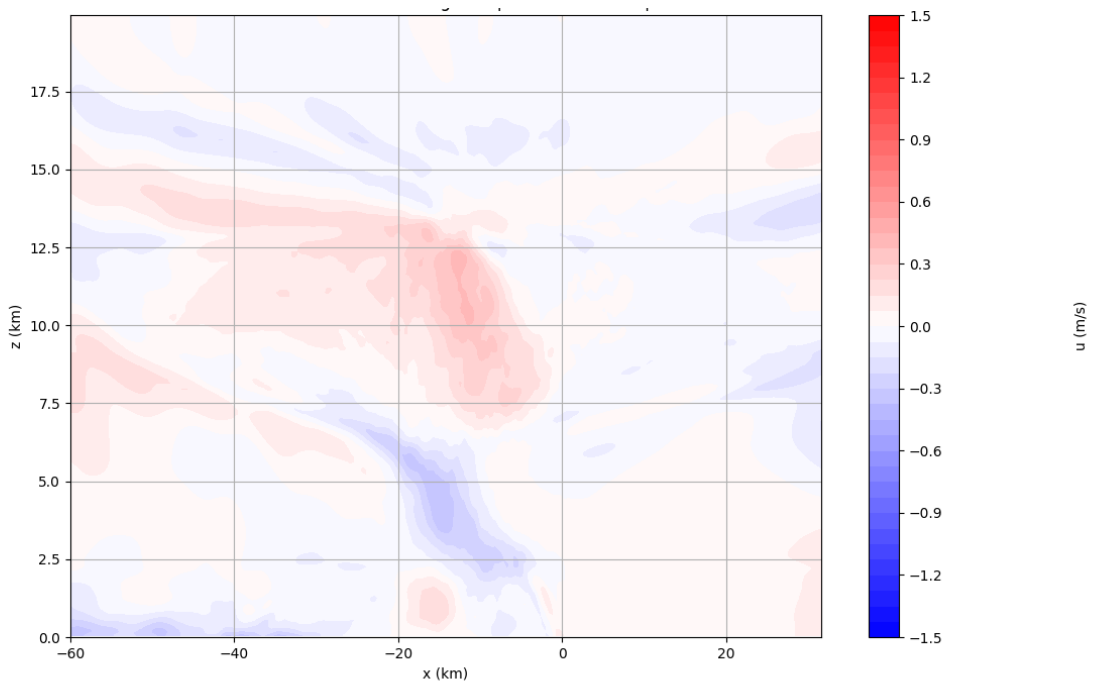
90 min:



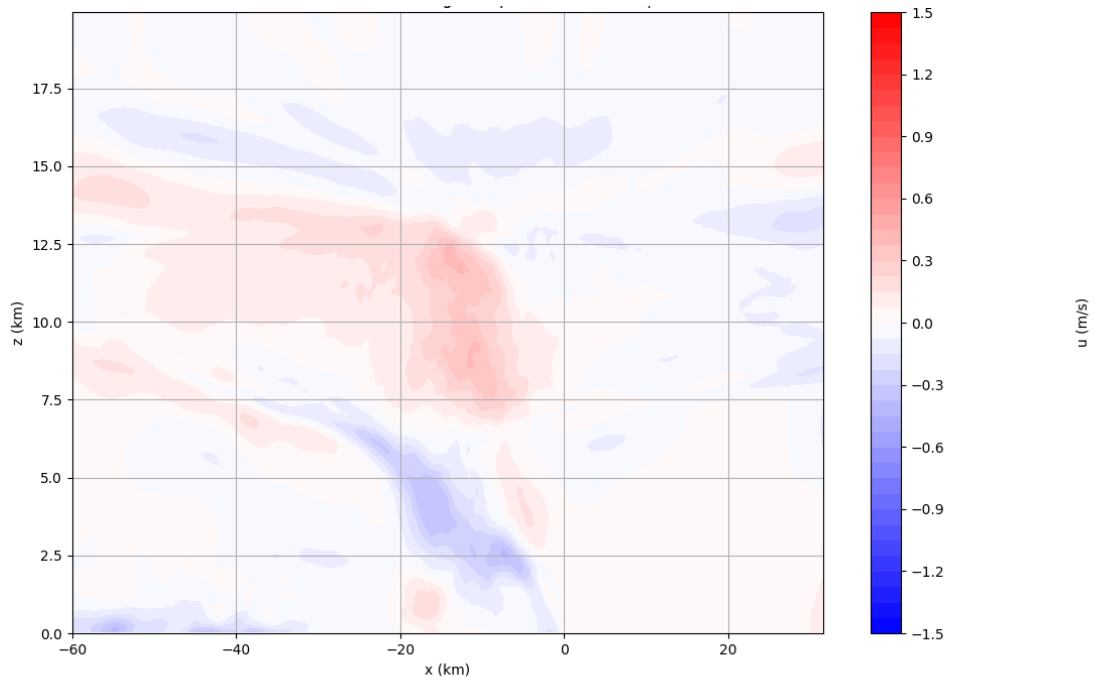
95 min:



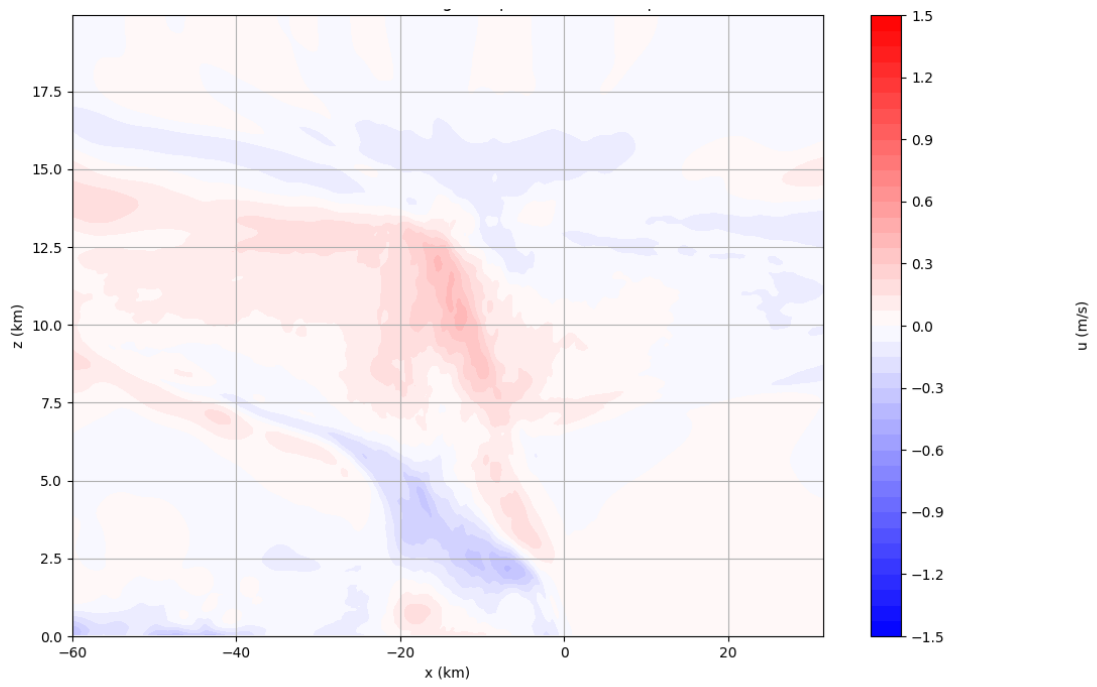
100 min:



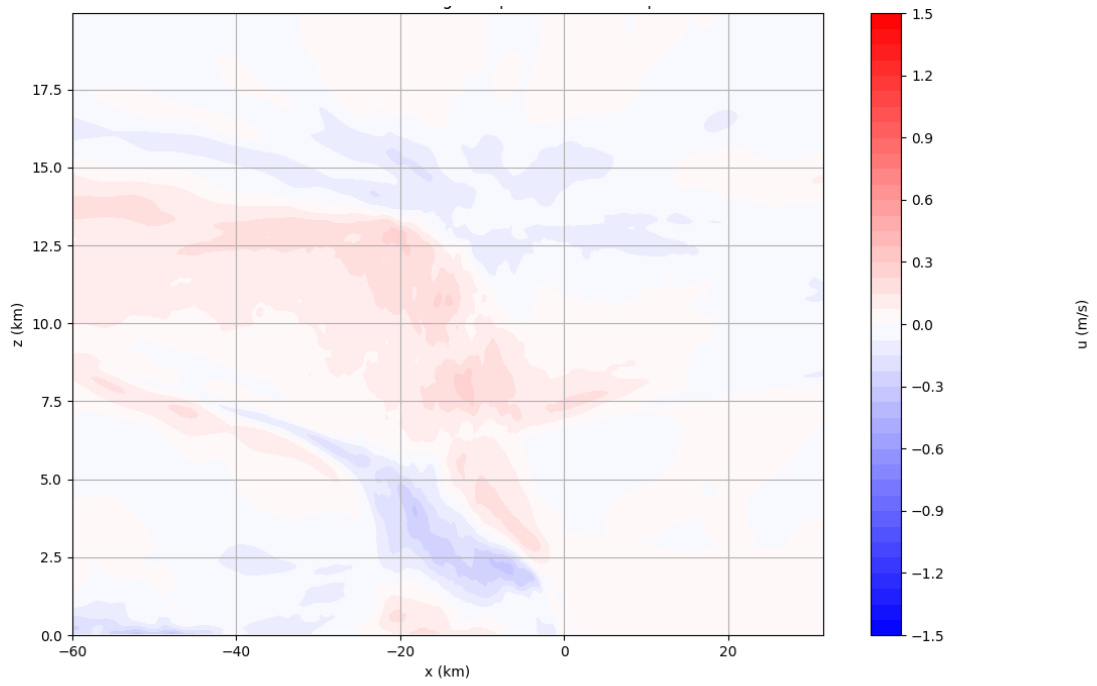
105 min:



110 min:



115 min:



120 min:

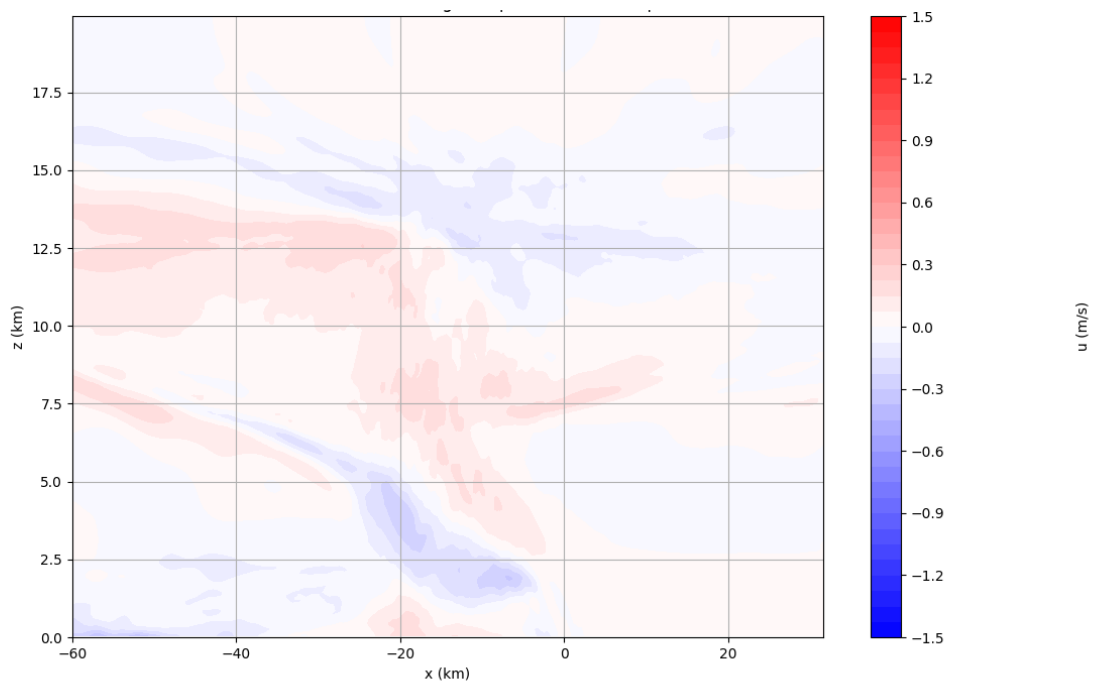
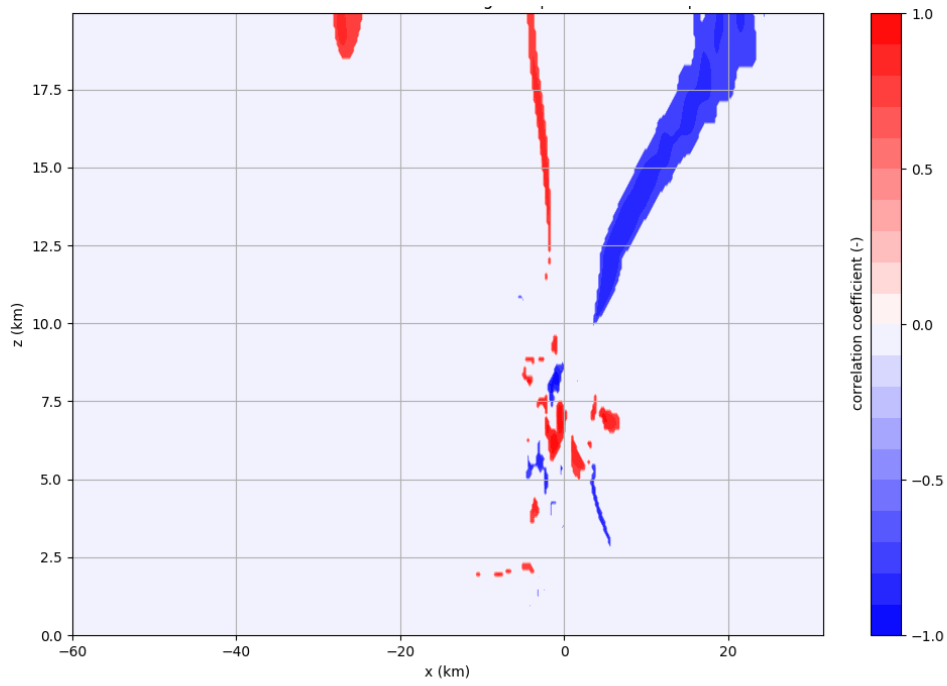
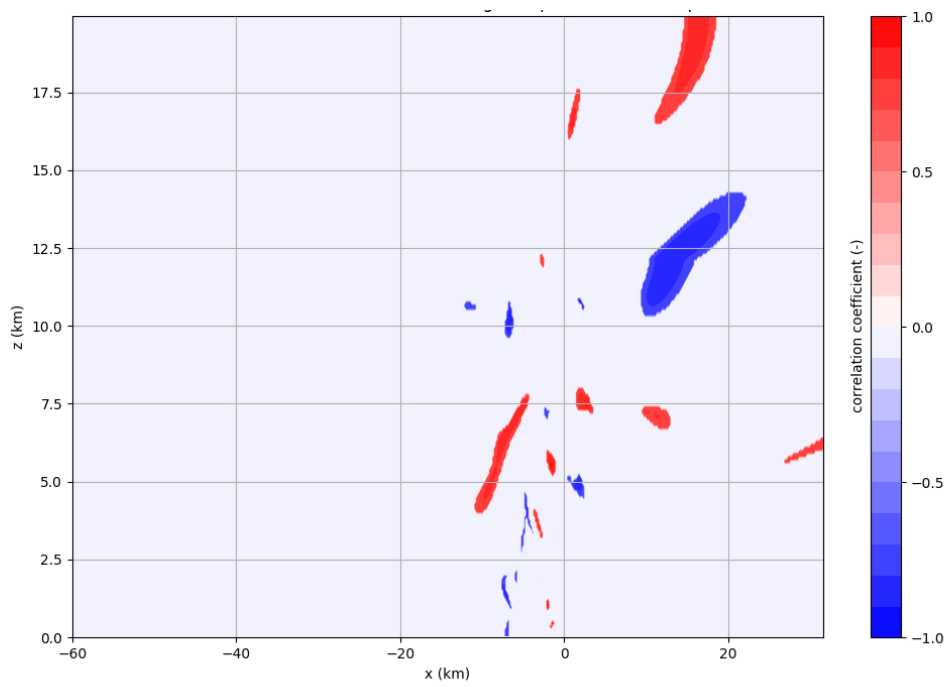


Figure S10 series: Masked correlations resulting from ensemble sensitivity analysis, exceeding $\alpha = 0,05$ threshold.

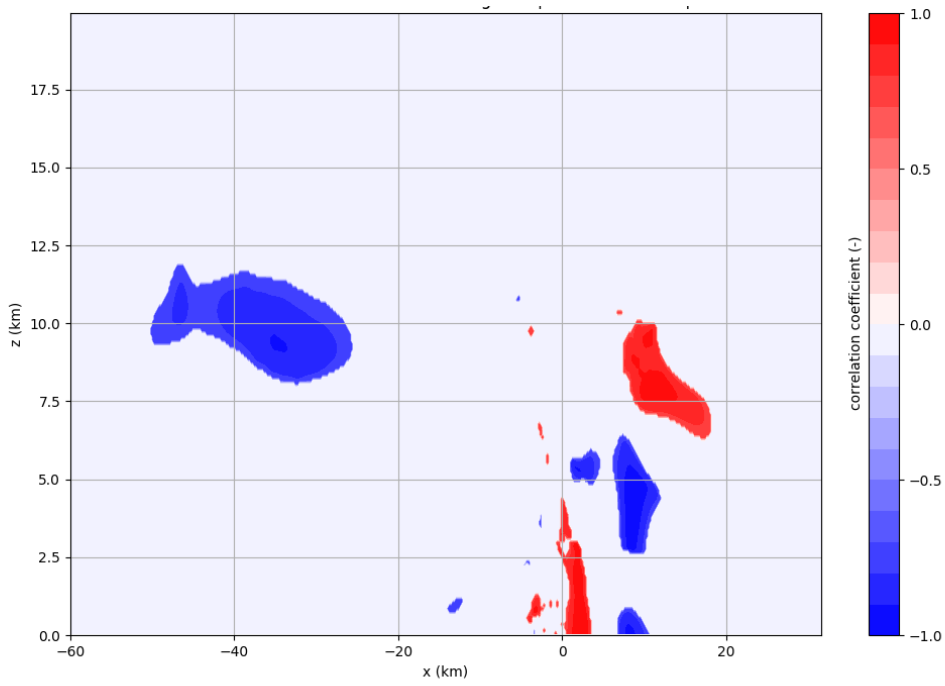
20 min:



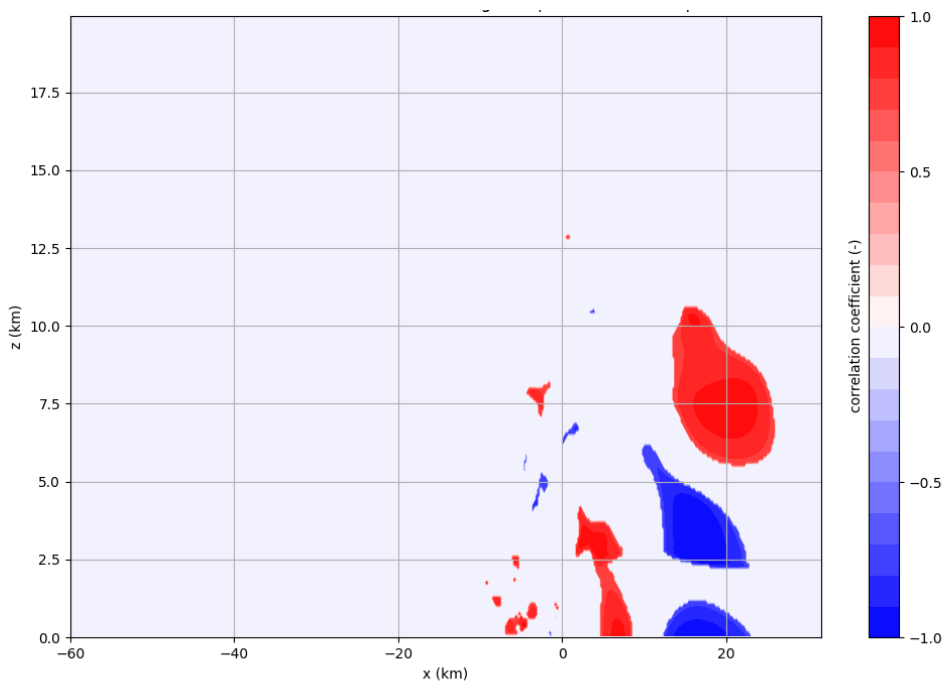
25 min:



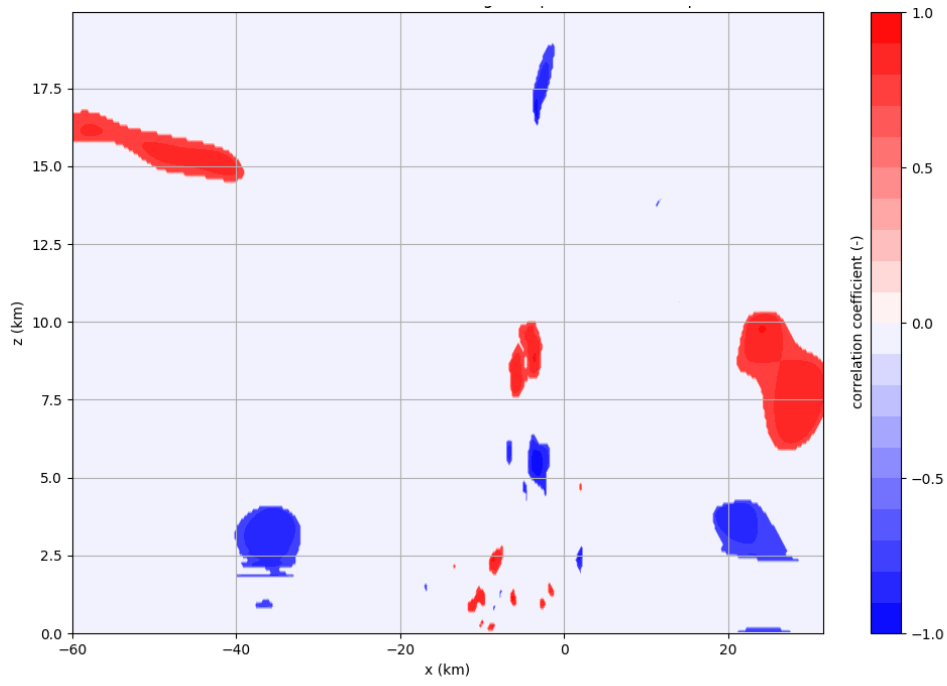
30 min:



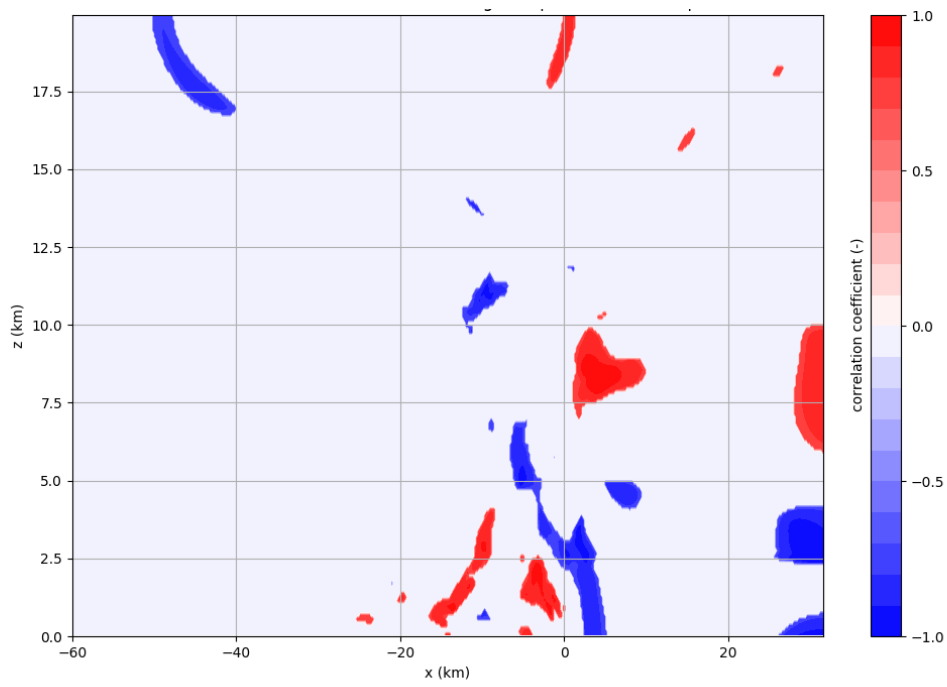
35 min:



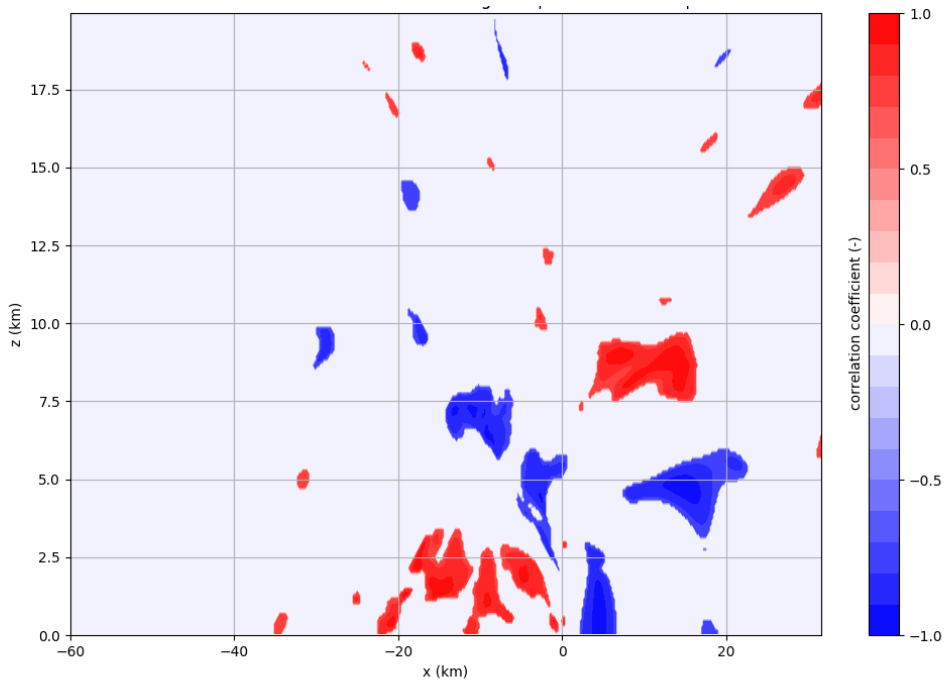
40 min:



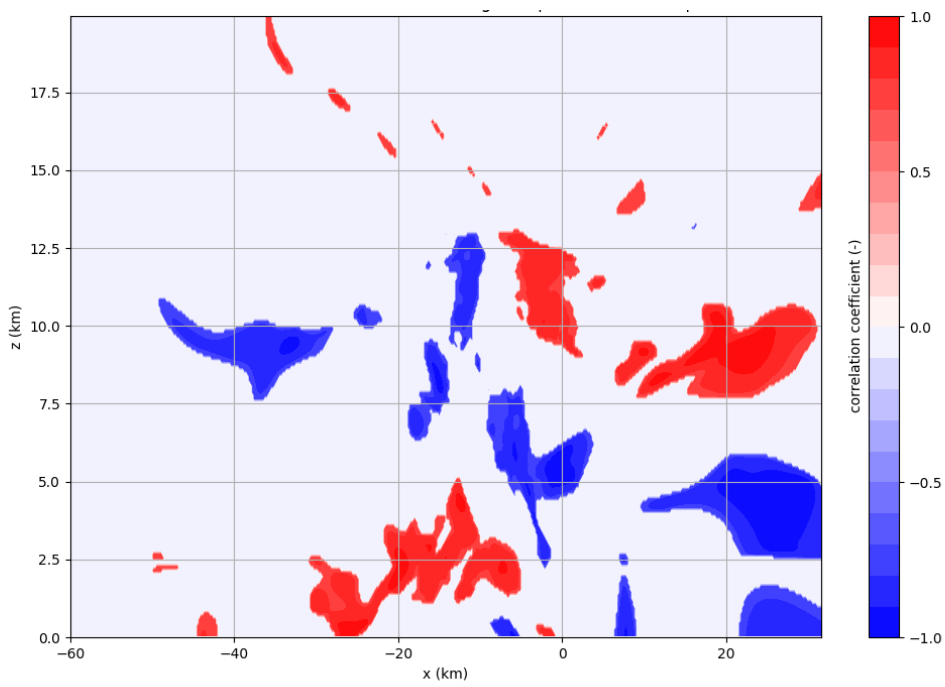
45 min:



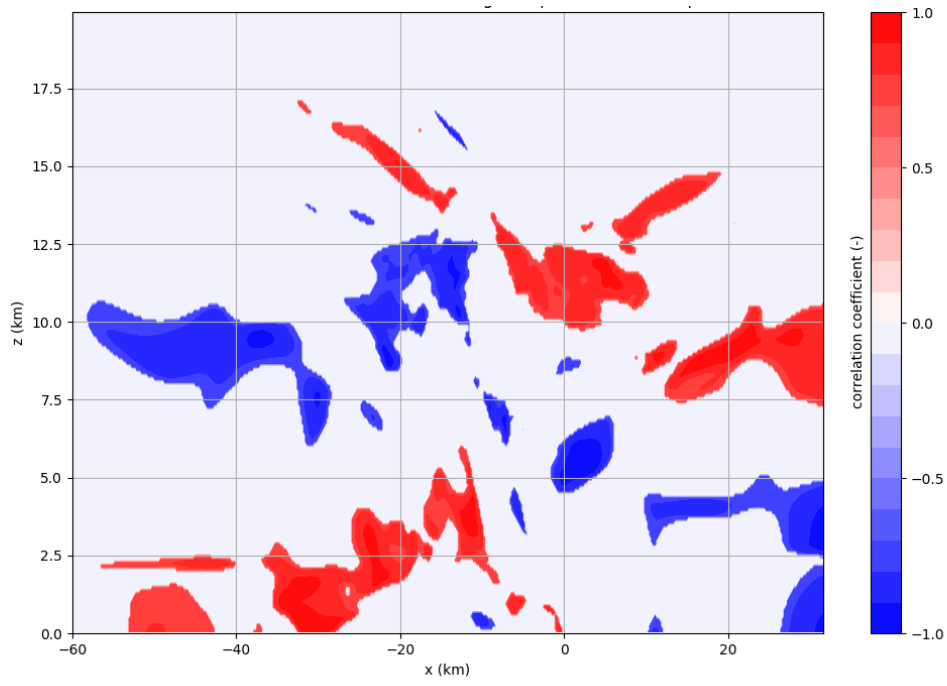
50 min:



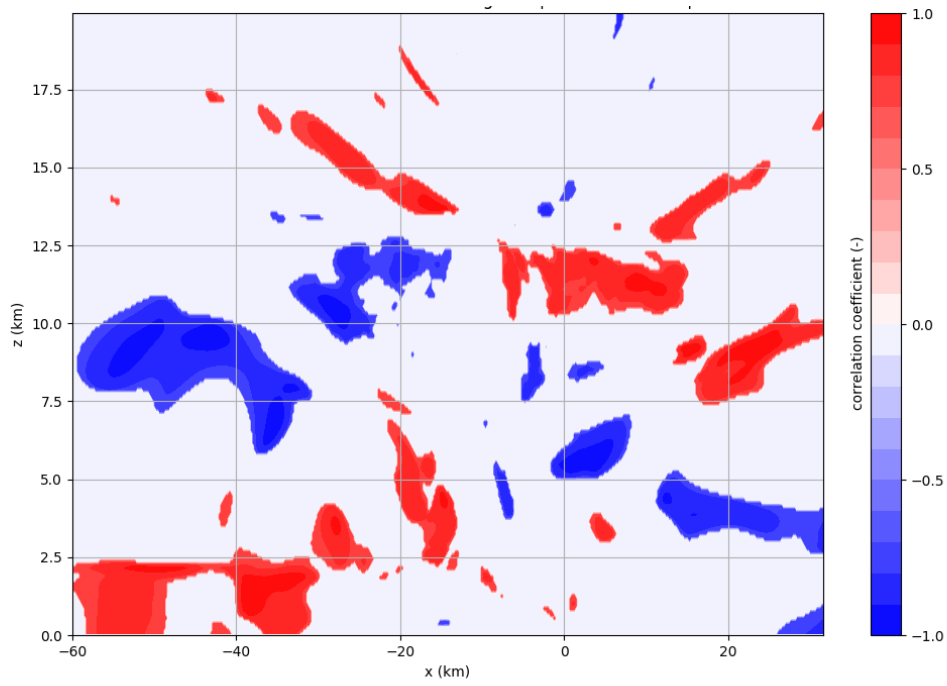
55 min:



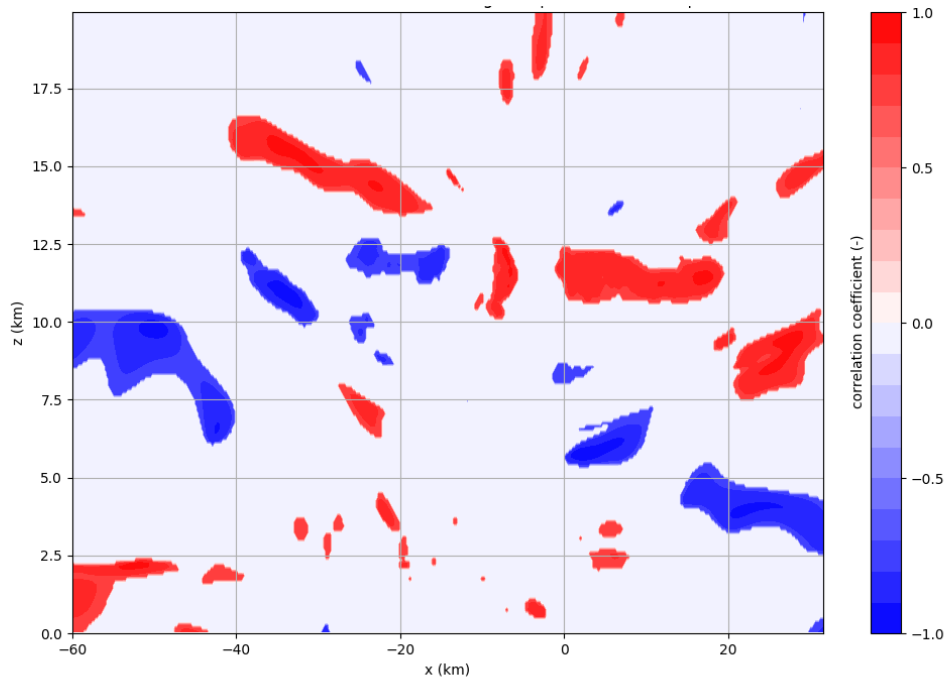
60 min:



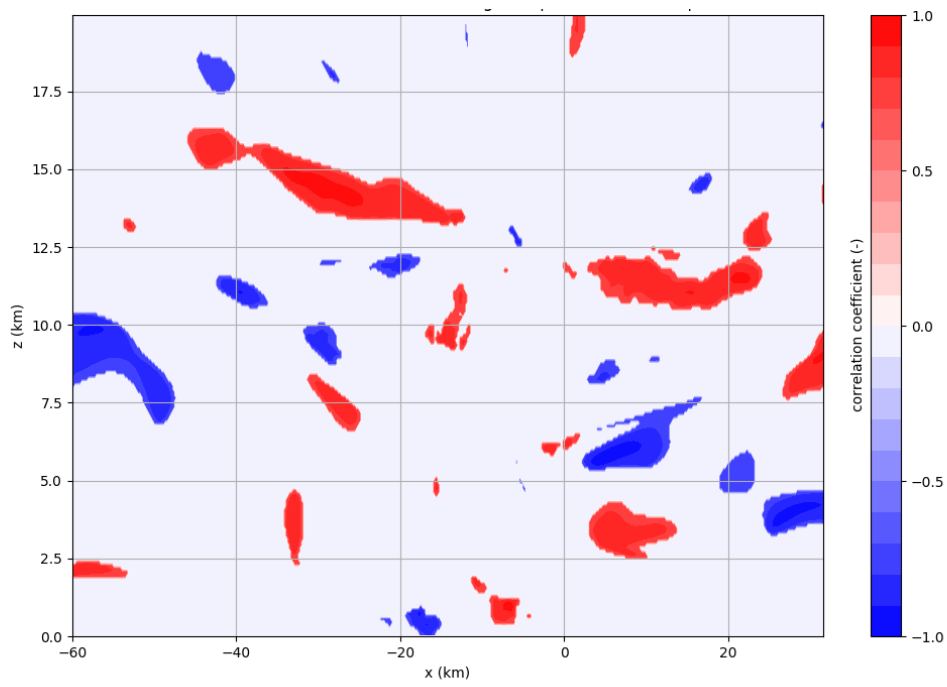
65 min:



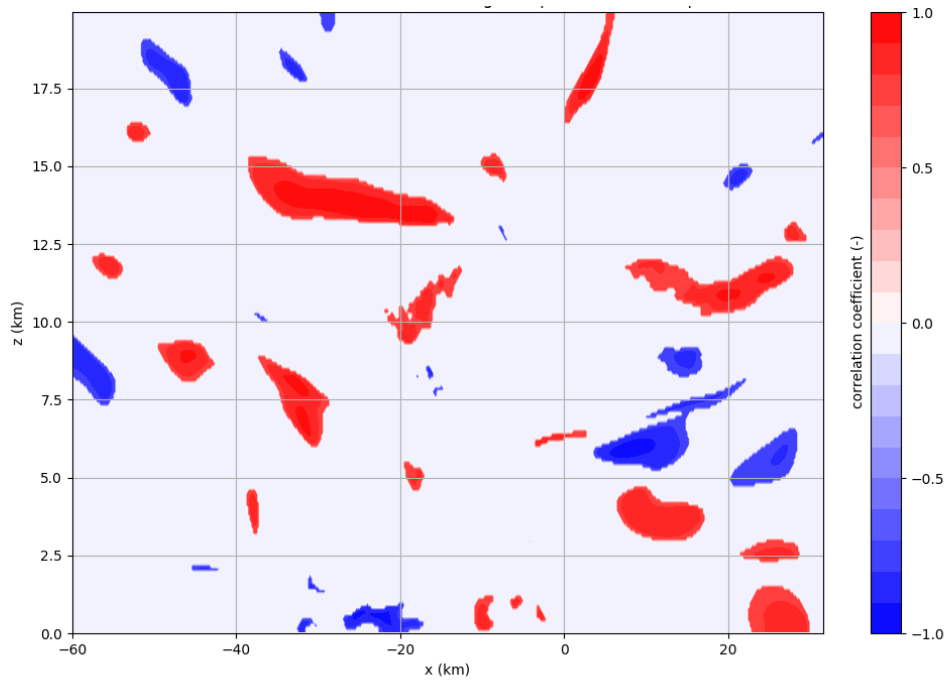
70 min:



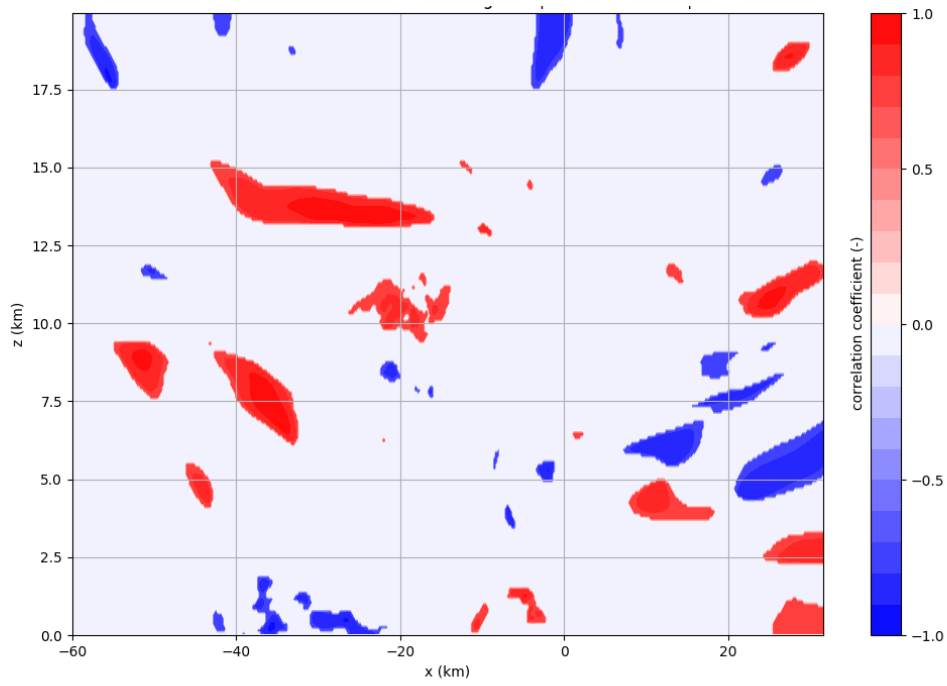
75 min:



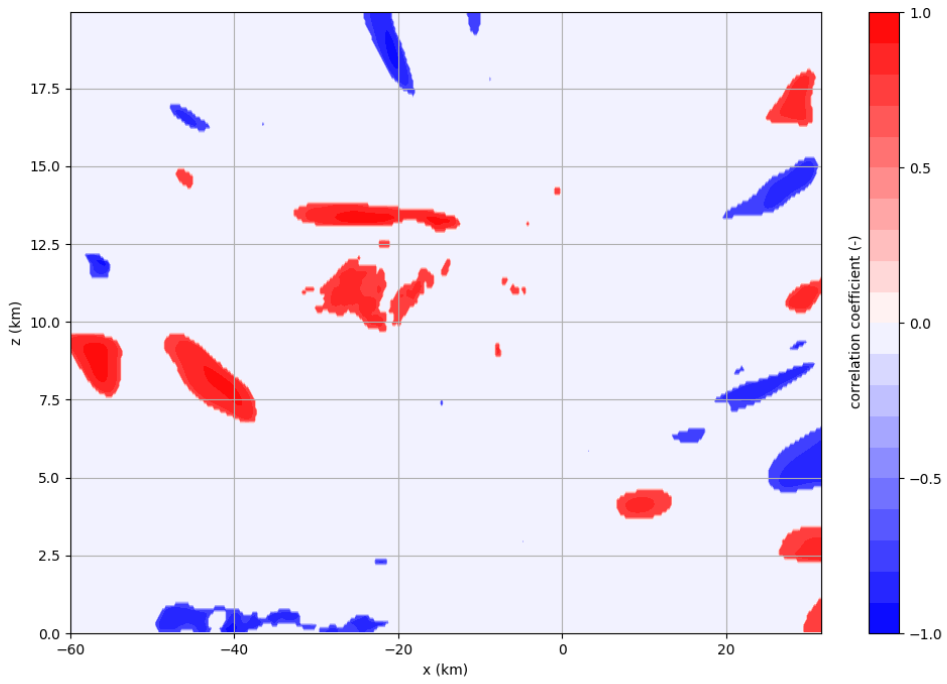
80 min:



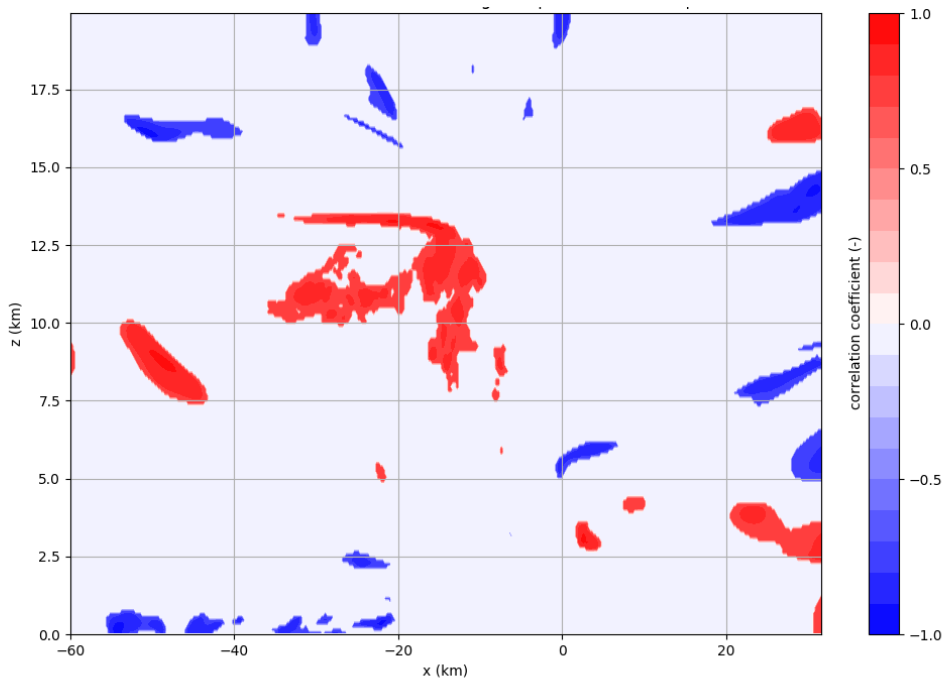
85 min:



90 min:



95 min:



100 min:

